

Abstract

Contents

1	Introduction	6
1.1	Overview	6
1.2	Transitional wall-bounded shear flows	9
1.2.1	Linear Stability Analysis	9
1.2.2	Nonlinear dynamical systems	13
1.2.3	Spatiotemporal transitional flows	16
1.3	Rayleigh-Bénard convection	19
1.4	Rayleigh-Bénard Poiseuille (RBP) flows	24
1.4.1	Thesis Outline	26
2	Numerical Techniques	28
2.1	Method of weighted residuals	28
2.2	Galerkin Projection	30
2.3	Spectral/ <i>hp</i> element method	32
2.3.1	Domain partition	32
2.3.2	Standard Elements	32
2.3.3	Global assembly	34
2.3.4	Local basis expansions	36
2.3.5	Gaussian quadrature	39
2.3.6	Numerical differentiation	40
2.3.7	Example in 1D	41
2.4	Numerical techniques for solving the Navier-Stokes equations	43
2.4.1	Velocity Correction Scheme	43
2.4.2	Fourier spectral/ <i>hp</i> modes	45
2.4.3	Maintaining fluid flow through a channel	46
2.5	Stability analysis of the Navier-Stokes equations	50
2.5.1	Algorithms for linear stability analysis	50
2.5.2	Edge tracking	54
3	Transitional Rayleigh-Bénard Poiseuille flows	57
3.1	Introduction	57
3.1.1	Rayleigh-Bénard Poiseuille (RBP) flows	57

3.1.2	Rayleigh-Bénard convection (RBC)	58
3.1.3	Plane Poiseuille flows (PPF)	59
3.1.4	Objectives and organisation	59
3.2	Problem formulation	60
3.2.1	Governing equations	60
3.2.2	Numerical Methods	60
3.2.3	<i>Ra-Re</i> sweep	61
3.2.4	Linear Stability Analysis	61
3.3	<i>Ra-Re</i> Phase Space	62
3.3.1	Classification	62
3.3.2	Spatiotemporal intermittent rolls	64
3.3.3	Coexistence with turbulent bands	66
3.4	The role of longitudinal rolls	68
3.4.1	The thermally-assisted sustaining process (TASP) in a confined domain	68
3.4.2	Variation of <i>Ra</i> and <i>Re</i> on the thermally sustained turbulent process within $\Gamma = \pi/2$	75
3.4.3	Extending to large domains, $\Gamma = 4\pi$	79
3.5	Conclusions	82
4	The state space structure of Spiral Defect Chaos	84
4.1	Introduction	84
4.1.1	Multiple convection states	84
4.1.2	Spiral defect chaos	85
4.1.3	Scope of this study	86
4.2	Problem formulation	87
4.2.1	Rayleigh-Benard convection (RBC)	87
4.2.2	Numerical method	87
4.2.3	Linear stability analysis of ISRs	88
4.3	Transient SDC and elementary states in minimal domain	89
4.4	Multiplicity of edge states	95
4.5	Unstable ideal straight rolls	100
4.5.1	Pathways leading to ISRs - heteroclinic orbits	104
4.5.2	Pathways leading to elementary states	107
4.5.3	A pathway to SDC in an extended domain $\Gamma = 4\pi$	109
4.6	Concluding remarks	114
5	Conclusions	116
A	Appendices	117
A.1	Non-dimensionalisation	117
A.2	Governing equations for Rayleigh-Bénard convection	117

A.3	Projection methods for Navier-Stokes equations	118
A.4	Simulation parameters for Ra - Re sweep	119
A.5	First- and second-order statistics of the buoyancy- and shear-driven regime	121
A.5.1	Buoyancy-driven regime	121
A.5.2	Shear-driven regime	121
A.6	Growth rates of primary instabilities	125
A.7	Verification of linear stability analysis	125
A.8	Other elementary states and ISRs	126

Chapter 1

Introduction

1.1 Overview

Fluid motions driven by buoyancy and frictional forces belongs to broad class of flows known as thermoconvective shear flows. These flows exhibit rich behaviour, and are of interest in both engineering and meteorology applications spanning across a broad range of length scales. At small scales, around $L \sim 1\text{cm}$, the thermoconvection flows are relevant to the cooling of microprocessing chips. In such systems, the fluid acts medium to dissipate heat, experiences shear forces from the confining walls, and buoyancy from heating. One of the major innovation in this industry is in squeezing more transistors onto a single chip, resulting to a doubling of transistors on a single chip roughly every two years, according to Moore's law. However, one of the major limitations on further miniaturisation is the challenge of dissipating the excessive heat generated. Fluids, such as air, water or refrigerant, are often used to transport heat away from the components, thereby preventing overheating [Kennedy and Zebib, 1983, Ray and Srinivasan, 1992]. At intermediate length scales, $L \sim 1\text{m}$, the interaction between buoyancy and frictional forces is important in the fabrication of uniform thin films in chemical vapour deposition (CVD) [Evans and Greif, 1991, Jensen et al., 1991]. The CVD process typically involves a reactive gases carried by inert gases which flows through a channel with a heated substrate. Upon heating, the reactant gases react chemically at substrate and deposits material, forming thin films, such as silicon layers. A key challenge in the CVD process is achieving a uniform deposition and maintaining sharp interfaces between layers. The interactions between shear and buoyancy forces often gives rise to boundary layers and thermoconvective rolls, which can disrupt uniform deposition, affecting film quality. At large scales, $L \sim 1\text{km}$, the thermoconvective shear flows can be observed in the atmosphere such as the cloud streets over the Norwegian Sea. These parallel bands of cumulus clouds can stretch over hundreds of kilometres. They form when relatively warm sea surfaces heat up the colder air blowing from the North [nor]. As the colder air is heated, it rises upwards whilst carrying water vapour. As it reaches a certain altitudes, $L \sim 1 - 10\text{km}$, the water vapour condenses into visible clouds, while the cooler air falls towards the sea. This circulation is organised into parallel rotating parallel columns of air, forming distinct cloud streets.

The common thread among the examples discussed above is the interaction between shear and buoyancy forces driven fluid motion - the central focus of this thesis. By restricting our analysis to these

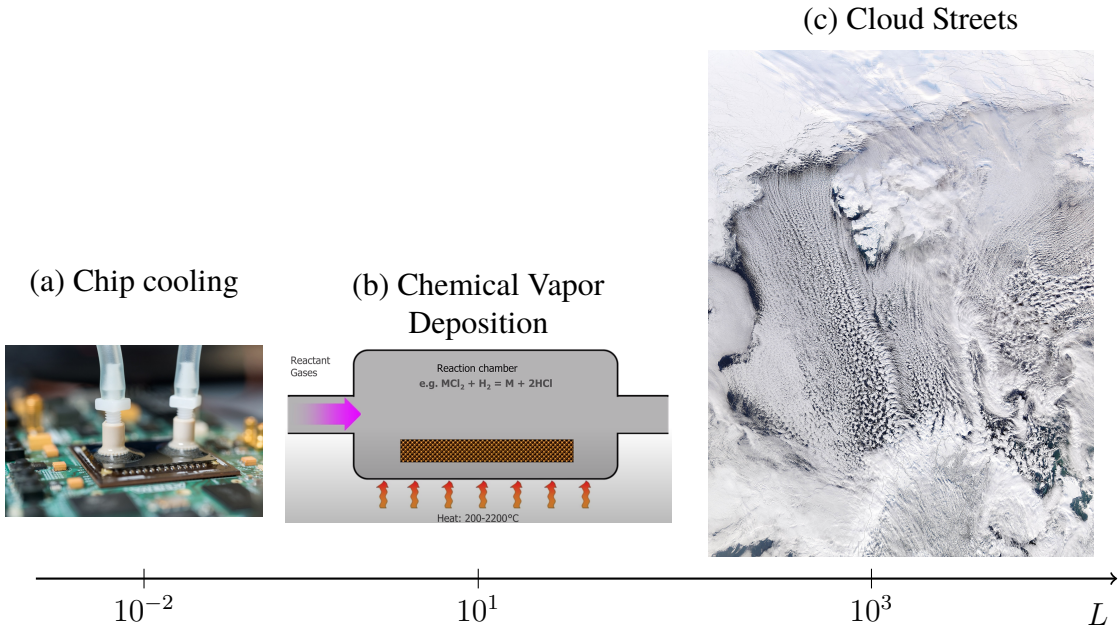


Figure 1.1: Fluid flow due to shear and buoyancy forces across length scales, $L \in [1\text{cm}, 1\text{km}]$, such as (a) chip cooling, (b) chemical vapour deposition and (c) formation of cloud streets.

two mechanisms, we neglect other physical mechanisms such as phase change, chemical reactions and evaporation, which may be significant in the context of cooling microprocessors, chemical vapour deposition, and atmospheric boundary layers respectively [Vallis et al., 2019]. To consider this interaction, we consider an idealised setup without geometric complexity, known to as the Rayleigh-Bénard-Poiseuille (RBP) flow. This system describes the fluid motion confined between two infinitely extended parallel plates, heated from below and cooled from the top, with an additional pressure gradient driving the flow. The RBP configuration combines two paradigmatic flow configurations; the classical Rayleigh-Bénard convection (RBC), driven purely by buoyancy, and plane Poiseuille flow (PPF), driven purely by shear. While the onset of convection in RBC, and the transition to subcritical shear-driven turbulence in PPF have been both extensively studied, the transitional regime in which both forces interact remains less understood. Gaining insights into this regime can have implications for various applications across a range of scales mentioned previously.

The RBP configuration is illustrated in figure 1.1, where $z^*, y^*, x^*, L_z, L_x, d, h$ refer to the streamwise, spanwise, wall-normal coordinates, length, span, depth and half-height of the domain respectively. We note that the asterisks*, refer to variables in dimensional form. The flow is driven by a pressure gradient along the streamwise z^* direction, $\Delta P^* = P^*|_{z^*=0} - P^*|_{z^*=L_z} < 0$, leading to the formation of a laminar Poiseuille flow, $w^*(y^*)$, for a sufficiently small ΔP . In this study, we will only consider fully-developed flow, where the boundary layer from the top and the bottom wall meets at the midplane, $y^* = 0$, and entrance effects are neglected. The RBP configuration is also unstably stratified, such that the temperature difference between the lower, T_L , and upper wall, T_U , is always positive, $\Delta T = T_L - T_U > 0$, leading to a stable linear conduction profile along the wall-normal direction, $T(y^*)$, if ΔT is kept sufficiently small.

In the absence of a pressure gradient, the RBP configuration reduces to the classical Rayleigh-

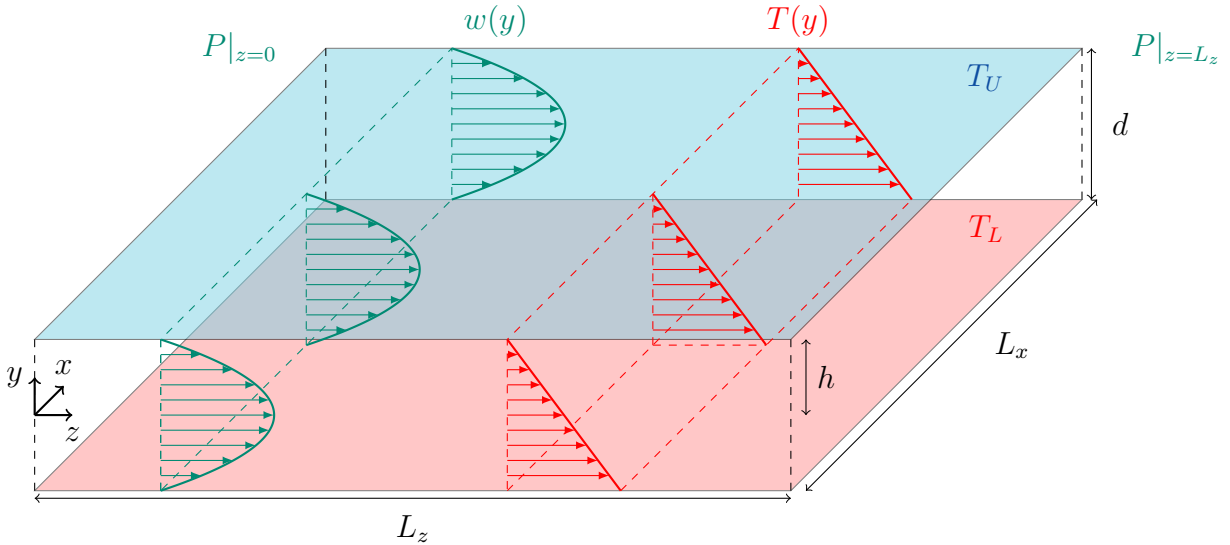


Figure 1.2: The Rayleigh-Bénard Poiseuille (RBP) flow configuration.

Bénard convection problem, bringing about buoyancy-driven convection for a sufficiently large unstable stratification. In the limiting case without unstable stratification, $\Delta T = 0$, the system reduces to the wall-bounded plane Poiseuille flow (PPF), where the transition towards subcritical shear-driven turbulence may be expected for a sufficiently large pressure gradient.

For instance, do buoyancy forces promote the transition to shear-driven turbulence and how does shear influence the convection? To describe the motion of the fluid in RBP configurations, we consider the non-dimensionalised Navier-Stokes equations with Boussinesq approximations,

$$\frac{\partial \mathbf{u}}{\partial t} + (\mathbf{u} \cdot \nabla) \mathbf{u} = -\nabla p + \frac{1}{Re} \nabla^2 \mathbf{u} + \frac{Ra}{Re^2 Pr} \theta, \quad (1.1a)$$

$$\frac{\partial \theta}{\partial t} + (\mathbf{u} \cdot \nabla) \theta = \frac{1}{Re Pr} \nabla^2 \theta, \quad (1.1b)$$

$$\nabla \cdot \mathbf{u} = 0. \quad (1.1c)$$

where $\mathbf{u}(\mathbf{x})$, $\theta(\mathbf{x})$, $p(\mathbf{x})$ refers to the nondimensionalised velocity, temperature and pressure respectively. The key control parameters for RBP flows are the Rayleigh number, Ra , Reynolds number, Re , Prandtl number Pr , which are defined as follows,

$$Ra = \eta g d^3 \Delta T / \nu \kappa, \quad Re = W_c h / \nu, \quad Pr = \kappa / \nu, \quad \Gamma = L / 2d, \quad (1.2)$$

where η , g , ΔT , ν , κ , W_c , h , d , L are the thermal expansion coefficient, acceleration due to gravity, temperature difference between the bottom and top wall, kinematic viscosity, thermal diffusivity, laminar centreline velocity, domain's half-depth, full-depth, length or span respectively.

We describe important historical of hydrodynamic stability of planar shear flows and their theoretical frameworks in §1.2. Theoretical frameworks used in the study of stability of flow such as linear stability, nonlinear dynamical systems and spatiotemporal character of transitional shear flows

will be outlined. This followed the historical developments of Rayleigh-Bénard convection (RBC), where concepts of the stability of fluid flows will be utilised in §1.3. After which, we describe the historical developments of RBP flows §1.4, and the outline of the thesis will be provided in §1.4.1.

1.2 Transitional wall-bounded shear flows

Wall-bounded shear flows concerns the motion of the fluid flowing in parallel to walls, typically bounded by one or more walls. Near the wall, the fluid comes to rest due to the no-slip boundary condition, resulting in a velocity gradient perpendicular to the wall, giving rise to shear within the fluid - hence the term *wall-bounded shear flows*. Examples include the pressure-driven plane Poiseuille flow (channel flow), Hagen-Poiseuille flow (pipe flow), plane Couette flow and flat plate boundary layers. These geometrically simple configurations provides a convenient framework amenable to the mathematical analysis of fluid motion subjected to shear. Depending on the degree of shear, the fluid motion can be either laminar, where the fluid layers move in smooth parallel 'laminates', or turbulent, characterised by chaotic eddying motions. We also note that there is a transitional regime where both states can coexist discuss later. A central question is predicting the transition from the laminar regime to the turbulence.

The first investigation into this transition was conducted by [Reynolds \[1883\]](#). In his experimental setup, the flow speed through the pipe could be controlled by regulating the inlet pressure, while injecting dye to visualise the flow, as illustrated in figure 1.3(a). At low speeds, the fluid remained laminar, resulting to a single streak of steady dye in figure 1.3(b). As the speed increased, the dye begin to exhibit irregular 'sinuous' motions interspersed with laminar regions shown in figure 1.3(c). This is now referred to as the transitional/intermittent regime, alternating between the laminar and turbulent states. Beyond a critical speed, the dye breaks down entirely into chaotic 'eddies', mixing with the surrounding fluid and discolouring the flow with dye downstream in figure 1.3(d). This regime is now identified as turbulence.

Reynolds proposed that the threshold between the laminar, transitional and turbulent regimes could be characterised by a non-dimensional parameter, now referred to as the Reynolds number,

$$Re = UD/\nu, \quad (1.3)$$

where U is the centerline velocity in the pipe, D , the pipe diameter and ν , the kinematic viscosity. He observed that flow through the pipe remained 'stable' and laminar for $Re < 1900$, while it became 'unstable' and turbulent for $Re > 2000$ [[Reynolds, 1895](#)]. These findings introduced the concept of flow stability.

1.2.1 Linear Stability Analysis

Following Reynolds' experiment, interest towards the mathematical analysis of the stability of laminar flows grew in early 20st century. The mathematical approach typically begins by decomposing the velocity field, $\mathbf{u}(\mathbf{x}, t)$, into a laminar (base) state, $U(y)$, and the velocity perturbations, $\mathbf{u}'(\mathbf{x}, t)$, with

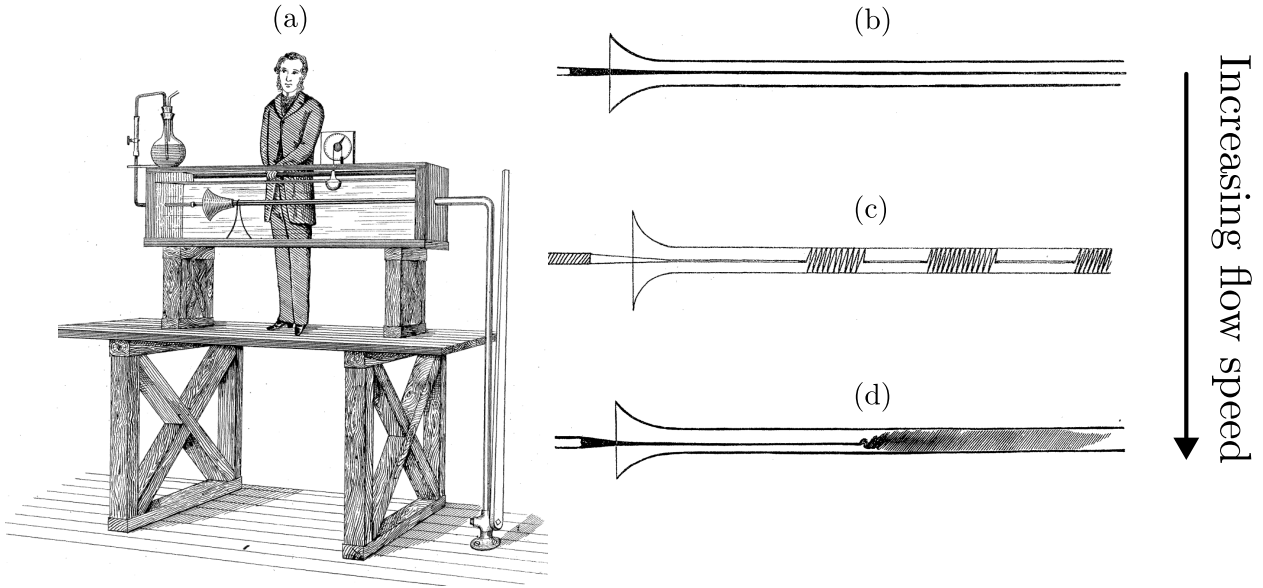


Figure 1.3: (a) Osbourne Reynolds pipe experiment with the dye injection apparatus, illustrating the (b) laminar flow, (c) intermittent regime and (d) turbulent flow as the flow speed is increased, taken from [Reynolds, 1883].

pressure similarly decomposed as,

$$\mathbf{u}(\mathbf{x}) = U(y) + \mathbf{u}'(\mathbf{x}, t), \quad \text{and} \quad p(\mathbf{x}, t) = P(x) + p'(\mathbf{x}, t). \quad (1.4)$$

Substituting into the Navier-Stokes equations and linearising (neglecting nonlinear terms), we get,

$$\frac{\partial \mathbf{u}'}{\partial t} + (U \cdot \nabla) \mathbf{u}' + (\mathbf{u}' \cdot \nabla) U = -\nabla p' + \frac{1}{Re} \nabla^2 \mathbf{u}', \quad (1.5a)$$

$$\nabla \cdot \mathbf{u}' = 0, \quad (1.5b)$$

known as the linearised Navier-Stokes equations. This commonly followed by introducing a wavelike ansatz (mode) defined by streamwise and spanwise wavenumbers, α, β and complex frequency, ω . In general two ways to analyse the linearised Navier-Stokes equations by considering the behaviour of each mode independently in §1.2.1 and their coupled dynamics in §1.2.1

Modal analysis

It is convenient to eliminate the pressure terms by reformulating equation (1.5) using the wall-normal perturbation velocity, v' , and wall-normal vorticity, $\eta' = \partial u'/\partial z - \partial w'/\partial x$, variables. Using (v, η) , we introduce a modal ansatz for them,

$$v'(\mathbf{x}, t) = \tilde{v}(y) e^{i(\alpha x + \beta z - \omega t)}, \quad \text{and} \quad \eta'(\mathbf{x}, t) = \tilde{\eta}(y) e^{i(\alpha x + \beta z - \omega t)}. \quad (1.6)$$

where α, β, ω denotes the streamwise and spanwise wavenumbers, and complex frequency (i.e. $\omega = \omega_r + i\omega_i$), respectively. Substituting this ansatz into linearised equations lead to the classical Orr-Sommerfeld and Squire equations [Orr, 1907, Sommerfeld, 1909, Squire, 1933, Schmid and Henningson, 2001],

$$\begin{pmatrix} \mathcal{L}_{OS} & 0 \\ i\beta U' & \mathcal{L}_{SQ} \end{pmatrix} \begin{pmatrix} \tilde{v} \\ \tilde{\eta} \end{pmatrix} = i\omega \begin{pmatrix} k^2 - \mathcal{D}^2 & 0 \\ 0 & 1 \end{pmatrix} \begin{pmatrix} \tilde{v} \\ \tilde{\eta} \end{pmatrix}. \quad (1.7a)$$

with

$$\mathcal{L}_{OS} = i\alpha U(k^2 - \mathcal{D}^2) + i\alpha U'' + \frac{1}{Re}(k^2 - \mathcal{D}^2)^2, \quad \mathcal{L}_{SQ} = i\alpha U + \frac{1}{Re}(k^2 - \mathcal{D}^2). \quad (1.7b)$$

where $\mathcal{D} = d/dy$, $k^2 = \alpha^2 + \beta^2$ and U'' is the second derivative of $U(y)$. Equation (1.7a) is an generalised eigenvalue problem with eigenvalue $i\omega$, which determines the growth of perturbations. The goal of modal stability analysis is to determine the critical Reynolds number Re_c , defined as the lowest value of Re , for all α and β in which $\Im[\omega] = 0$. For $Re > Re_c$, perturbations can grow exponentially, indicating instability. Squire's theorem states that for every unstable three-dimensional perturbation, there exist an unstable two-dimensional perturbation, with a lower Re_c [Squire, 1933]. This implies that the most linearly unstable perturbation of wall-bounded flows is two dimensional. Calculations by Tollmien [1928] and Schlichting [1933] for a flat-plate boundary layer flow yielded a critical Reynolds number based on streamwise distance x of $Re_{x,c} = Ux_c/\nu = 520$ [Schlichting and Gersten, 2017]. These two dimensional unstable eigenmodes are known as Tollmien-Schlichting (T.S) waves. In plane Poiseuillw flow, the critical Reynolds number is $Re_c = 5772.2$ with a critical wavenumber of $\alpha_c = 1.02$ [Orszag, 1971]. However, experiments reveal that transition to turbulence can occur at must lower Reynolds number, around, $Re \sim 1000 - 2000$ [Davies and White, 1928, Patel and Head, 1969, Dean, 1978, Iida and Nagano, 1998, Tsukahara et al., 2014a], highlighting a key limitation of modal analysis. Similar discrepancies are observed in plane Couette and pipe flows [Meseguer and Trefethen, 2003], where the laminar state is linearly stable for all Re , yet transition to turbulence occurs. Despite these limitations, modal analysis predicts instabilities in other flows such as Rayleigh-Bénard convection and Taylor-Couette flow [?]. Further developments, including spatial instability analysis [?], and secondary instability [?] are beyond the scope of this thesis.

Non-modal stability

One of a major limitations of modal analysis is that it treats each eigenmode independently. However, the interaction between decaying eigenmodes can lead to a transient growth, where perturbations amplify temporarily before decaying asymptotically. To demonstrate an example of transient growth, we consider a two-dimensional toy model governing the time-evolution of \mathbf{q} ,

$$\frac{d}{dt} \begin{pmatrix} v \\ \eta \end{pmatrix} = \begin{pmatrix} -\frac{1}{Re} & -1 \\ 0 & -\frac{2}{Re} \end{pmatrix} \begin{pmatrix} v \\ \eta \end{pmatrix}, \quad (1.8)$$

where Re refers to the Reynolds number. The toy model is has negative eigenvalues, $(\lambda_1, \lambda_2) = (-1/Re, -2/Re)$, indicating asymptotic decay. At $Re = 15$, the eigenvectors, $\mathbf{x}_1 = (1, 0)$, $\mathbf{x}_2 =$

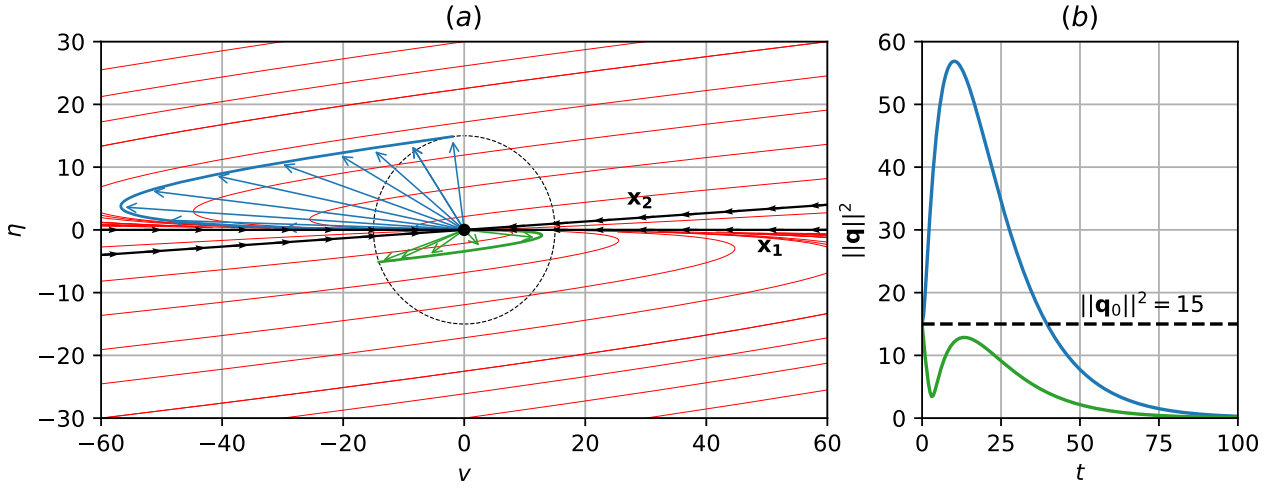


Figure 1.4: (a) The phase portrait of the toy model with $Re = 15$, where red lines are phase lines of the toy model. The blue trajectory lead to transient growth and the green trajectory do not (b) Time history of blue and green trajectory.

$(1, \frac{1}{\sqrt{Re^2+1}})$, are highly non-orthogonal, becoming almost linear dependent as shown in figure 1.4(a). Notably, we become increasingly linearly dependent as $Re \rightarrow \infty$. For a particular initial condition, the energy $\|q\|^2 = \sqrt{v^2 + \eta^2}$, is amplified four times before decaying in blue trajectory, shown in Figure 1.4(b). Yet for another choice of initial condition, the trajectory decays asymptotically as the green trajectory indicates. Despite decaying eigenmodes, the toy model highlights the significance of transient growth, which depends on the choice of initial condition.

The aim of non-modal stability analysis is find the initial conditions, $\tilde{\mathbf{q}}_0$, that leads to the maximum amplification, $G(\tau)$, over a time horizon τ . This is posed as an optimistaion problem,

$$G(\tau) = \max_{\tilde{\mathbf{q}}_0 \neq 0} \frac{\langle \tilde{\mathbf{q}}(\tau), \tilde{\mathbf{q}}(\tau) \rangle}{\langle \tilde{\mathbf{q}}_0, \tilde{\mathbf{q}}_0 \rangle}, \quad \text{s.t. } \langle \tilde{\mathbf{q}}_0, \tilde{\mathbf{q}}_0 \rangle = 1, \quad (1.9)$$

where, $\langle \cdot, \cdot \rangle$ denotes the inner-product,

$$\langle \mathbf{x}, \mathbf{y} \rangle = \int_{\Omega} \mathbf{x}^H \mathbf{y} \, d\Omega, \quad (1.10)$$

and \mathbf{x}^H refers to the complex conjugate transpose of \mathbf{x} . By considering the linearised operator of (1.7a), we can define a linear time invariant operator given as,

$$\tilde{\mathbf{q}}(\tau) = \mathcal{A}(\tau) \tilde{\mathbf{q}}_0, \quad (1.11)$$

which takes the solution from initial conditions, $\tilde{\mathbf{q}}_0$, to $\tilde{\mathbf{q}}(\tau)$ at time τ . Subtituting the expression above into equation (1.9),

$$G(\tau) = \max_{\tilde{\mathbf{q}}_0 \neq 0} \frac{\langle \mathcal{A}(\tau) \tilde{\mathbf{q}}_0, \mathcal{A}(\tau) \tilde{\mathbf{q}}_0 \rangle}{\langle \tilde{\mathbf{q}}_0, \tilde{\mathbf{q}}_0 \rangle} = \langle \tilde{\mathbf{q}}_0, \mathcal{A}^\dagger(\tau) \mathcal{A}(\tau) \tilde{\mathbf{q}}_0 \rangle = \lambda_{max}(\mathcal{A}(\tau)^\dagger \mathcal{A}(\tau)) \quad (1.12)$$

where \mathcal{A}^\dagger refers to the adjoint of $\mathcal{A}(t)$. The maximum amplification factor $\max G(t)$ is the largest eigenvalue of $\mathcal{A}^\dagger(\tau)\mathcal{A}(\tau)$. The eigenvalue problem is given as,

$$\mathcal{A}^\dagger(t)\mathcal{A}(t)\tilde{\mathbf{q}}_0 = \lambda\tilde{\mathbf{q}}_0, \quad (1.13)$$

where $\tilde{\mathbf{q}}_0$ refers to the eigenvector denoting the optimal initial condition. For a detailed derivation of the optimal initial conditions or forcing, the reader is referred to [Butler and Farrell, 1992, Schmid, 2007]. An alternative method of computing transient growth is computing the pseudospectral of linear operators discussed in [Trefethen, 1997], outside the scope of this thesis.

Both two-, and three-dimensional non-modal analyses reveal mechanisms for transient growth. In two-dimensions, the optimal initial conditions are in the form of near wall vortices tilted upstream, which amplifies via the Orr-mechanism [Orr, 1907, Farrell, 1988, Reddy et al., 1993]. In three-dimensions, streamwise vortices are optimal, leading to the the amplification of streamwise streaks via the lift-up effect [Ellingsen and Palm, 1975, Reddy and Henningson, 1993]. The spacing of these streaks at higher Reynolds number has been consistently reported to occur around 100 wall units [Del Álamo and Jiménez, 2006, Pujals et al., 2009, Hwang and Cossu, 2010], which supports experimental observations of streak spacing in turbulent boundary layers [Kline et al., 1967, Smith and Metzler, 1983]. The main results from non-modal analysis is that three dimensional perturbations can lead to strong transient growth at subcritical Reynolds numbers while modal analysis predicts the onset of two-dimensional instabilities via Tollmien Schlichting waves.

Both modal and non-modal mechanisms highlight important developments, providing perspectives on linear mechanisms responsible for the transition from laminar to turbulence.

1.2.2 Nonlinear dynamical systems

In the previous section, we have examined the laminar to turbulent transition using linear frameworks. However, the the transition process is ultimately described by the nonlinear Navier-Stokes equations, which motivates the development and adoption of mathematical frameworks beyond linear methbods. In the context of shear flow turbulence, there has been a growing interesting in adopting techniques from nonlinear dynamical systems, interpreting turbulence as a chaotic trajectories which evolves within a finite-dimensional phase space. This phase space refers to a set of solutions satisfying the Navier-Stokes equations, conjectured to be infinite dimensional by Hopf [1948]. Hopf [1948] further conjectured that within the infinite dimension phase space lie a finite dimensional manifold, whose properties depended on viscosity. For large viscosities (i.e. low Re), this finite dimensional space corresponds to a single point, the laminar state. This point may become unstable at a certain critical Reynolds number, bifurcating to form new manifolds, as viscosity is decreased (i.e. Re is increased) further, potentially leading to chaos. The set of such manifolds is referred to *inertial manifolds*, and its existence is established under certain properties [Foias et al., 1988]. A implication of this is the transition to turbulence could be viewed as successive bifurcations govern by a single control parameter (i.e. the Reynolds numnber), described by the so called *routes to chaos* scenarios. Landau [1944] proposed that the transition to turbulence may occur through a sequence of Hopf bifurcations,

each introducing a new incommensurate frequency, resulting in quasi-periodic motions on a high-dimensional torus. However, this model did not capture the essential ingredients of turbulence, such as sensitivity of initial conditions and mixing [John et al., 1993]. Ruelle and Takens [1971] later show that a *strange attractor* exhibit key features of chaos can emerge after three successive Hopf bifurcations from a stationary state, referred to as the *Ruelle-Takens* route to chaos. This scenario has been have been observed in Taylor-Couette flow [Gollub and Swinney, 1975], and Rayleigh-Bénard convection Swinney and Gollub [1978]. Other routes to chaos such as periodic-doubling [Feigenbaum, 1979], and intermittency Manneville and Pomeau [1979] scenarios have been proposed. For a review of these routes to chaos scenarios, the reader is referred to John et al. [1993]. Nonetheless, the transition to turbulence is subcritical in shear flow configurations, meaning that the route of chaos scenarios do not necessarily apply through bifurcations from the laminar state.

In the adoption of nonlinear dynamical systems of wall-bounded shear flows, a major development came with the identification of a pair of non-trivial, unstable equilibrium states in plane Couette flow [Nagata, 1990]. This pair referred to as the *lower* and *upper* branches, emerging from a saddle node bifurcation which is disconnected from the stable laminar state. The *lower* branch lies closer to the laminar state, while the *upper* branch resides further away in state space. Later, a travelling-wave solution in plane Couette flow also later found by the same author [Nagata, 1997]. A family of equilibrium and travelling-wave solutions was found later for plane Couette and plane Poiseuille flows under different boundary conditions (i.e. stress-free, slip and no-slip) were identified by [Waleffe, 2001, 2003], sometimes referred to as *exact coherent states*. Additional equilibria and travelling-wave solutions were identified by Gibson et al. [2008, 2009], along with their heteroclinic connections between them [Halcrow et al., 2009]. In the context of pipe flow, multiple travelling-wave solutions have also been reported [Faisst and Eckhardt, 2003, Wedin and Kerswell, 2004, Kerswell and Tutty, 2007, Wang et al., 2007, Duguet et al., 2008, Pringle et al., 2009]. The set of equilibria, and travelling waves, shows good agreement with the statistical quantities (e.g. mean and fluctuations) with direct numerical simulations. However, since they are equilibria, and travelling-waves (relative equilibria), they do no capture the temporal dynamics of turbulence such as the *self-sustaining process* (SSP) [Hamilton et al., 1995]. While these unstable solutions demonstrate good agreements with results from DNS such as the spanwise length scales, and mean and fluctuations, they do not capture the dynamical processes.

The next breakthrough was on the idenfitification of time-dependent invariant solutions in the form of periodic orbits. Kawahara and Kida [2001] computed a pair of periodic orbits in plane Couette, with one exhibiting a single regeneration cycle similar to the SSP while the other exhibits mild modulation of streaks. These periodic orbits are connected via heteroclinic trajectories. In plane Poiseuille flow, Toh and Itano [2003] also identified periodic orbits displaying bursting behaviour. Using a Newton–Krylov iteration with a hook-step modification, Viswanath [2007] computed multiply relative periodic orbits. These studies conceptualise that the chaotic trajectories of turbulence as being embedded within a set of unstable periodic orbits, evolving along their unstable manifolds [Viswanath, 2007, Gibson et al., 2008, 2009, Halcrow et al., 2009, Graham and Floryan, 2021]. An example is shown in figure 1.5, where the chaotic trajectories in figure 1.5(b), reside within the same state space as the periodic orbits,

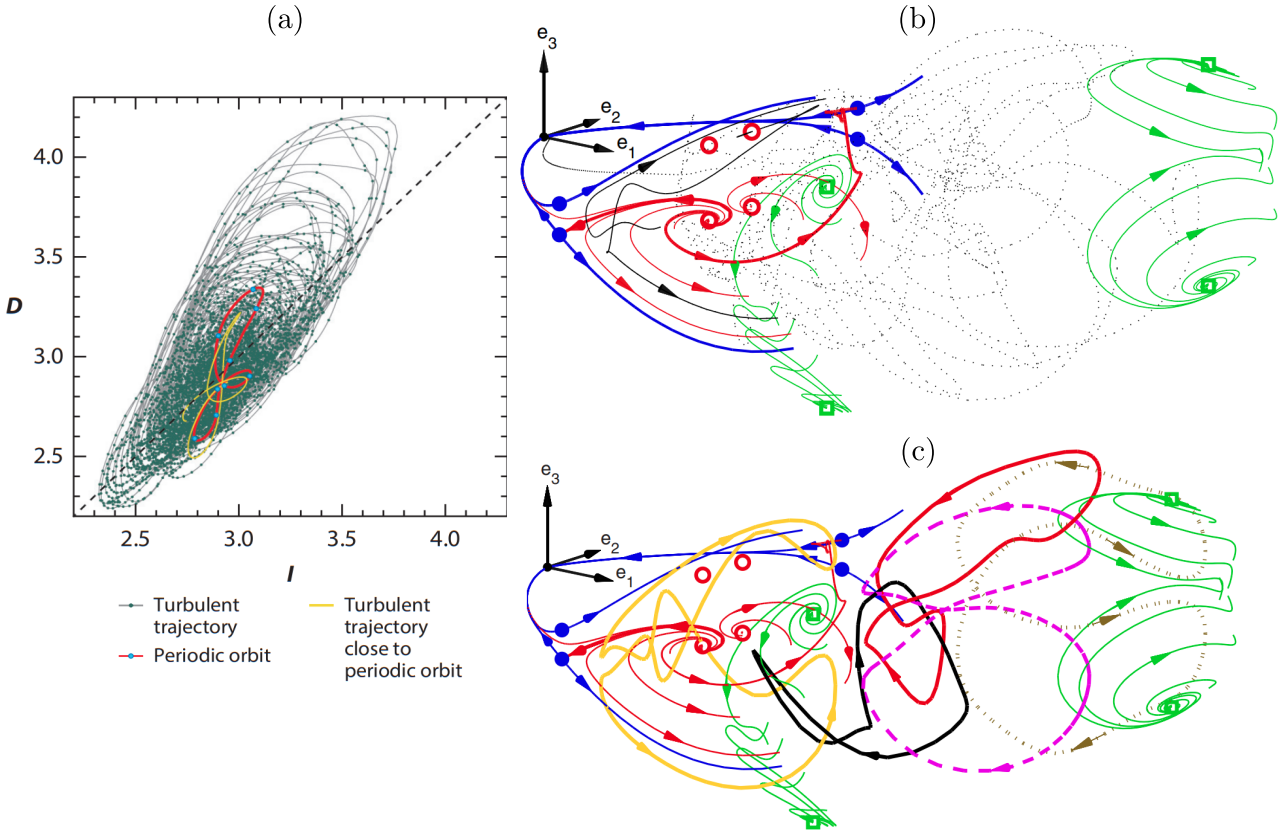


Figure 1.5: (a) Chaotic trajectories of turbulence of plane Couette flow at $Re = 400$, approaching the an unstable periodic orbit (red) highlighted as yellow, adopted from [Kawahara and Kida \[2001\]](#). (b) State space organisation of turbulence trajectories (black dots) confined around equilibria (circles, dots and squares) and their unstable manifolds (solid lines), heteroclinic connections between them are shown in red. The coordinate system is centered on the laminar state, using a linear combination of the upper branch invariant state. (c) State space projection of five periodic orbits (coloured solid lines), embedded within the same space where turbulence evolves in (b), adopted from [\[Cvitanović and Gibson, 2010\]](#).

enclosed by equilibria and their heteroclinic connections shown in figure 1.5(c). The set of equilibria, travelling waves and their relative counterparts, are referred to as *invariant solutions* offering an alternative view of the building blocks of turbulence. However, they do not provide insight into the transition process, since these solutions already reside in the turbulent regime.

The transition to turbulence in canonical shear flow configurations are typically subcritical, emerging from the invariant solutions described above, with an underlying stable laminar state. A consequence of this is that the laminar and turbulent states form a bistable attractors in phase space. The laminar and turbulent states coexist as stable attractors, with a boundary—known as the *edge*, separating their respective basins of attraction. Attractors that sit along this edge have been identified and found to possess a saddle-like structure, attracting trajectories within the edge and repelling them toward either the laminar or turbulent state, known as *edge states*. The algorithm to identify such states, known as edge tracking, was first employed in pipe flow experiments [Schneider et al. \[2007\]](#), where the it chaotic. Time-averaging of this chaotic attractor revealed a close resemblance to the unstable lower branch travelling-wave solutions, suggesting that the edge separating basin of attraction between

the laminar and turbulent states consist of the lower branch solutions and their symmetries [Duguet et al., 2008, Pringle et al., 2009]. As Reynolds number increases, the edge and the turbulent attractor move apart [Schneider and Eckhardt, 2009]. In the context of pipe flows, it was recognised that the edge consists of a set of unstable travelling-wave solutions connected to the lower branch. A graphical representation of the edge, and edge states, separating the laminar the turbulent states is shown in figure 1.6. Near the onset of subcritical turbulence, turbulence appear to be transient, decaying towards

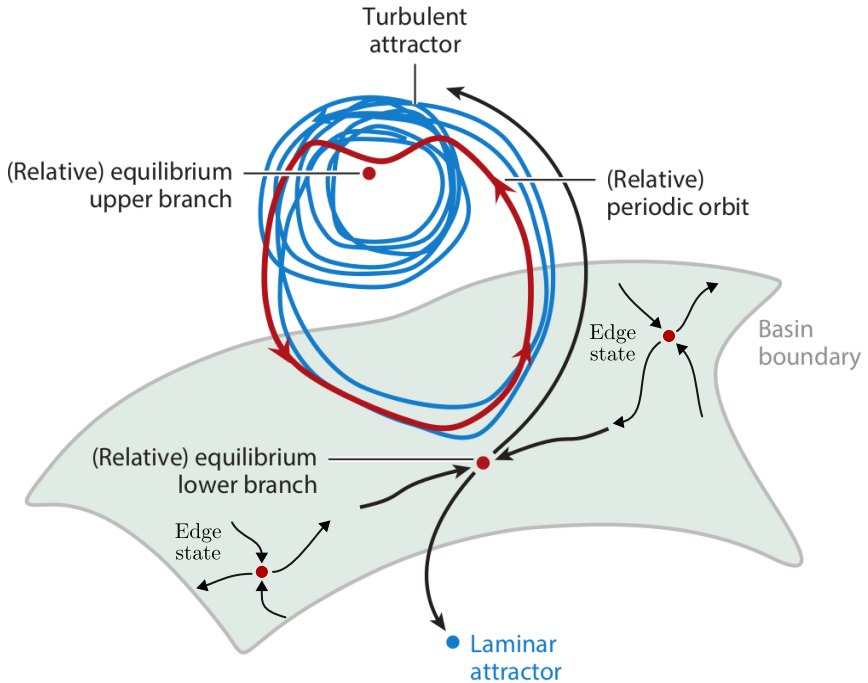


Figure 1.6: A graphical representation of the edge (grey surface) separating the basin of boundary of the laminar and turbulent attractor, consisting of attractors, known as edge states, adapted from Graham and Floryan [2021].

the laminar solution after a finite lifetime [Bottin et al., 1998, Faisst and Eckhardt, 2004, Hof et al., 2006] This may be interpreted as the turbulent attractor colliding with the lower branch solution (i.e. the edge) through a *boundary crisis* [Lai and Tél, 2011], where the chaotic attractor becomes *leaky*, providing an avenue for the solution trajectory towards relaminarisation [Kreilos and Eckhardt, 2012, Zammert and Eckhardt, 2015].

1.2.3 Spatiotemporal transitional flows

This section describes the inherent spatiotemporal structure of subcritical turbulence near the onset commonly reported in large extended domains. In this regime, turbulence is characterised by the coexistence of turbulent and laminar structures. Examples of such are found in canonical shear flow systems such as plane Couette flows [Prigent et al., 2003, Barkley and Tuckerman, 2005, 2007, Tuckerman and Barkley, 2011, Duguet et al., 2010, Reetz et al., 2019], Taylor-Couette flows [Prigent and Dauchot, 2002, Prigent et al., 2003], pipe flows [Avila et al., 2010, 2011, Song et al., 2017, Avila et al., 2023] and plane Poiseuille flows [Tsukahara et al., 2014a,c, Tuckerman et al., 2014, Tsukahara

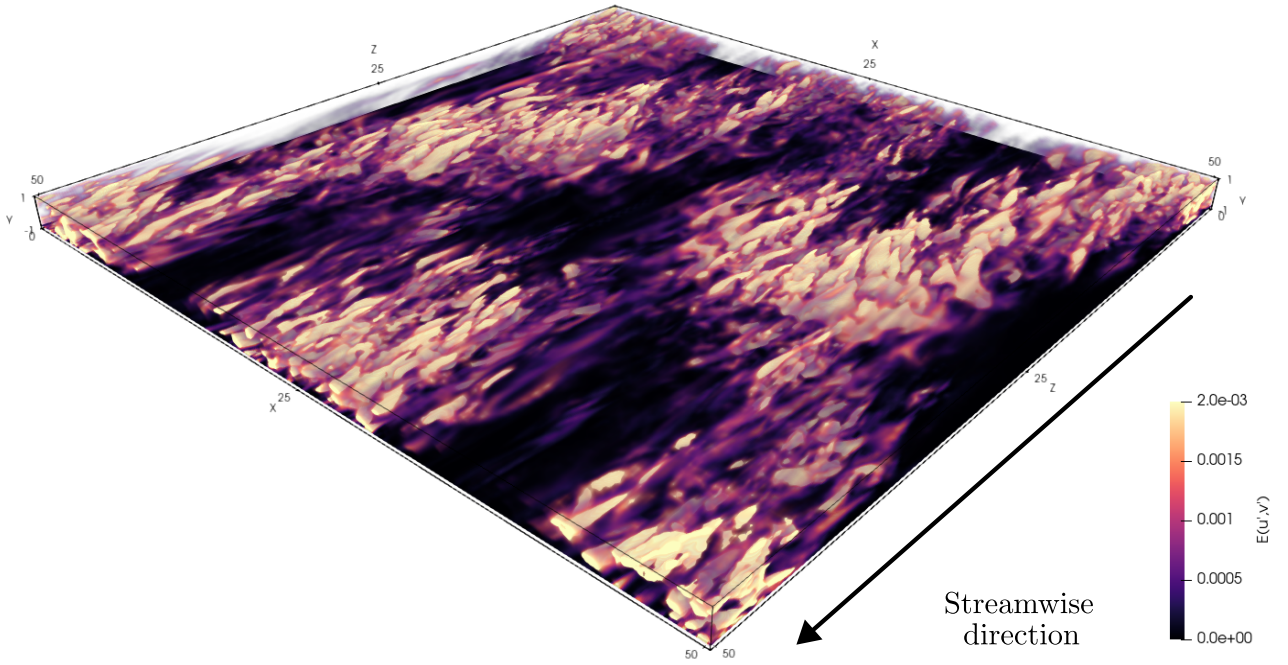


Figure 1.7: A snapshot of turbulent-laminar bands at $Re = 1400$ in a large domain $L/d = 8\pi$, depicting its spatiotemporal intermittent nature. Isovolumetric renderings are based on the spanwise, u' , and wall-normal, v' , perturbation kinetic energy, $E(u', v') = 1/2(u'^2 + v'^2)$, where the perturbation velocities are defined about the laminar state $\mathbf{u}'(\mathbf{x}, t) = \mathbf{u}(\mathbf{x}, t) - U_{lam}(y)$.

et al., 2014b, Gomé et al., 2020, Paranjape, 2019, Paranjape et al., 2020, 2023].

We will focus on the plane Poiseuille flow configuration, where the spatiotemporal intermittent patterns are referred to as oblique turbulent-laminar bands illustrated in figure 1.7 at $Re = 1400$ for $L/h = 16\pi$. The bright and dark regions highlight coexisting spatially localised turbulent and laminar regions. These turbulent-laminar bands occur over a range of Reynolds numbers, and its precise range is likely dependent on the domain's aspect ratio [Tsukahara et al., 2014b, Tuckerman et al., 2014, Paranjape et al., 2023]. Near the upper Re threshold of this regime, the domain is fully engulfed by developed turbulent regions, referred to uniform, featureless turbulence appearing at $Re = 1800$ in figure 1.7(a). As Re decreases towards $Re = 1050$, spatiotemporal turbulence characterised by turbulent and laminar structures known as turbulent-laminar bands persist in figures 1.8(b-f). In particular, these turbulent-laminar have a preferred inclined angle, between $20^\circ \sim 30^\circ$, with streamwise wavelengths of $\sim 60h$, and spanwise wavelengths of $\sim 20h - 30h$ [Tsukahara et al., 2014b]. Kashyap et al. [2022] considered the linear response of the fluctuating turbulent field, and showed that the preferred band angle emerges near 23.2° . Below certain Re threshold, the spatially turbulent regions decay where the flow relaminarises [Tuckerman et al., 2014]. An example of this decay is shown in $Re = 1000$ near $t = 1600$ in figure 1.8(g).

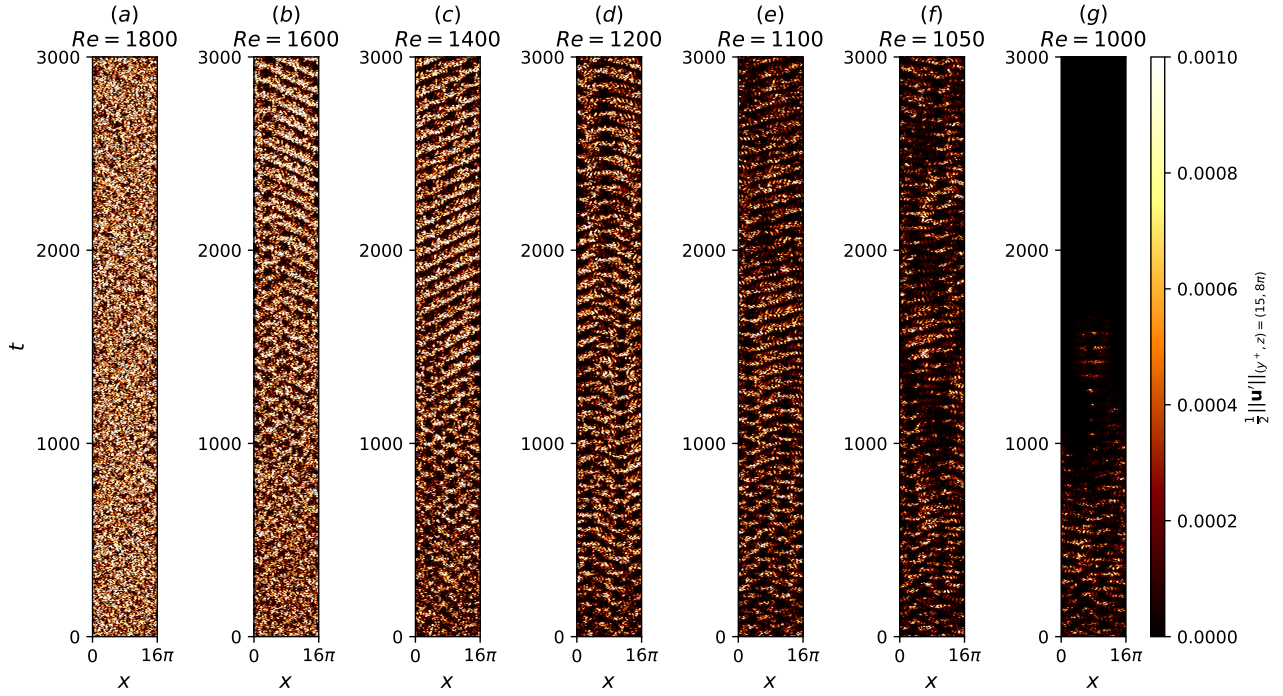


Figure 1.8: Turbulent-laminar bands for $t \in [0, 3000]$ in large domains $(L_x, L_z) = (16\pi, 16\pi)$ at (a) $Re = 1800$, (b) $Re = 1600$, (c) $Re = 1400$, (d) $Re = 1200$, (e) $Re = 1100$, (f) $Re = 1050$, (g) $Re = 1000$.

Inspired from previous studies of turbulent-laminar bands in plane Couette flows [Barkley and Tuckerman, 2005, Reetz et al., 2019], the minimal band unit (MBU) was employed for plane Poiseuille flows [Tuckerman et al., 2014, Paranjape et al., 2020, 2023]. In MBUs of plane Poiseuille flows, the turbulent-bands convect at about $\sim 1\%$ of the bulk velocity, propagating either upstream or downstream, above or below an critical $Re \sim 1000$, independent of domain sizes for $L_z \geq 100h$ [Tuckerman et al., 2014, Gomé et al., 2020]. The spanwise lengths of the bands are much wider than the half-heights, appearing at $\lambda_z \sim 20h$ for $Re \geq 1400$ and $\lambda_z \sim 40h$ for $Re \leq 1100$, suggesting that the characteristic spanwise lengths are dependent on Re . Interestingly, the bands alternate between both spanwise lengths between the Re range, merging and splitting continuously [Tuckerman et al., 2014], reminiscent of a puff splitting in pipe flows [Avila et al., 2011].

As Re is lowered, turbulent bands spontaneously decay and relaminarises [Tuckerman et al., 2014, Gomé et al., 2020]. Gomé et al. [2020] computed the probabilities distributions for turbulent-laminar band decay, $P(\Delta t^d)$, where Δt^d is the time until decay. A key insight is that the probability distributions of turbulent band decay mimics a memoryless Poisson process,

$$P(\Delta t^d) = \exp(-\Delta t^d/\tau^d(Re)), \quad (1.14)$$

where $\tau^d(Re)$ refers to the mean lifetime for decay as a function of Re . Similarly, the band splitting process also follow a Poisson process

$$P(\Delta t^s) = \exp(-\Delta t^s/\tau^s(Re)), \quad (1.15)$$

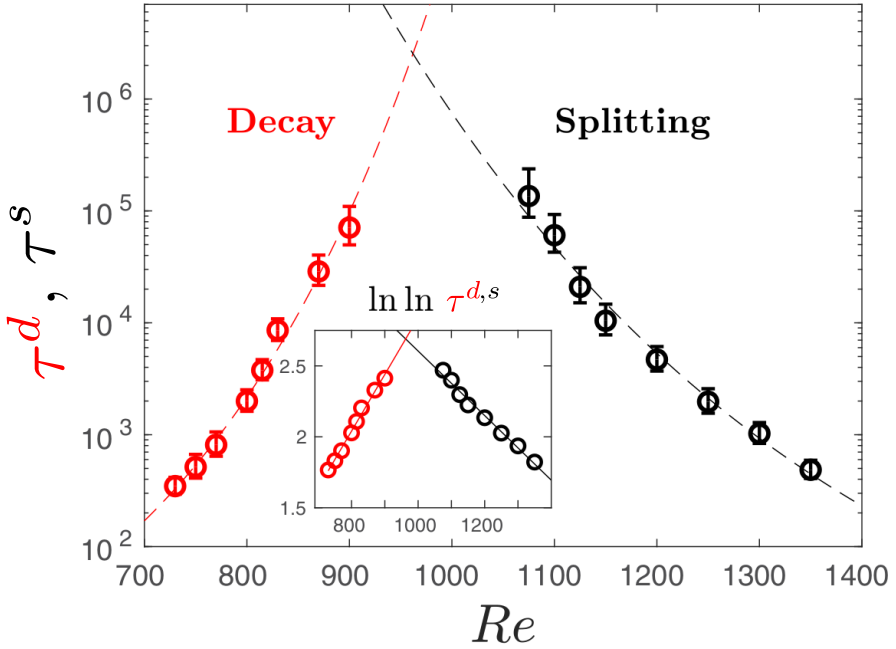


Figure 1.9: The mean decay times (red), τ^d , and mean splitting times (black), τ^s , as a function of Reynolds number, leading to a crossover point at $Re \approx 965$, adapted from [Gomé et al., 2020].

white $\tau^s(Re)$ the mean splitting lifetime. Both τ^d and τ^s exhibit superexponential dependence on Re ,

$$\tau^{d,s} = \exp(\exp(Re)), \quad (1.16)$$

This is shown in figure 1.9, with a crossover point at $Re_{cross} \approx 965$, where both decay and splitting becomes equally probable. This crossover point is considered as the critical Reynolds number for the onset of turbulent bands. While there has progress made towards understanding the behaviour of periodic turbulent-laminar bands MBUs, recent studies of isolated turbulent bands (ITBs) reveal different behaviour. Notably, ITBs persist at $Re \approx 700$ for duration exceeding $t = 10000$, far exceeding the ranges in figure 1.9. The ITBs are characterised by streak generating head and a diffusive upstream tail. [Xiong et al., 2015, Tao et al., 2018, Shimizu and Manneville, 2019, Xiao and Song, 2020]. We conclude our discussion on transitional wall-bounded shear flows.

1.3 Rayleigh-Bénard convection

Rayleigh-Bénard convection (RBC) is a paradigmatic fluid configuration describing the motion of the fluid confined between two infinite-parallel plates heated from below and cooled from the top. As the bottom plate is heated, the bottom layer fluid becomes more buoyant and tends to rise, while the colder top fluid layer becomes relatively less buoyant and tends to sink, leading to an overturning of layers. Viscous forces between neighbouring fluid parcels act to resist the motion. As buoyancy overcomes these viscous forces, the fluid layers overturn, resulting in the initiation of buoyancy-driven convection, the physical mechanism underpinning RBC.

One of the earliest experimental studies dedicated to buoyancy-driven convection was conducted

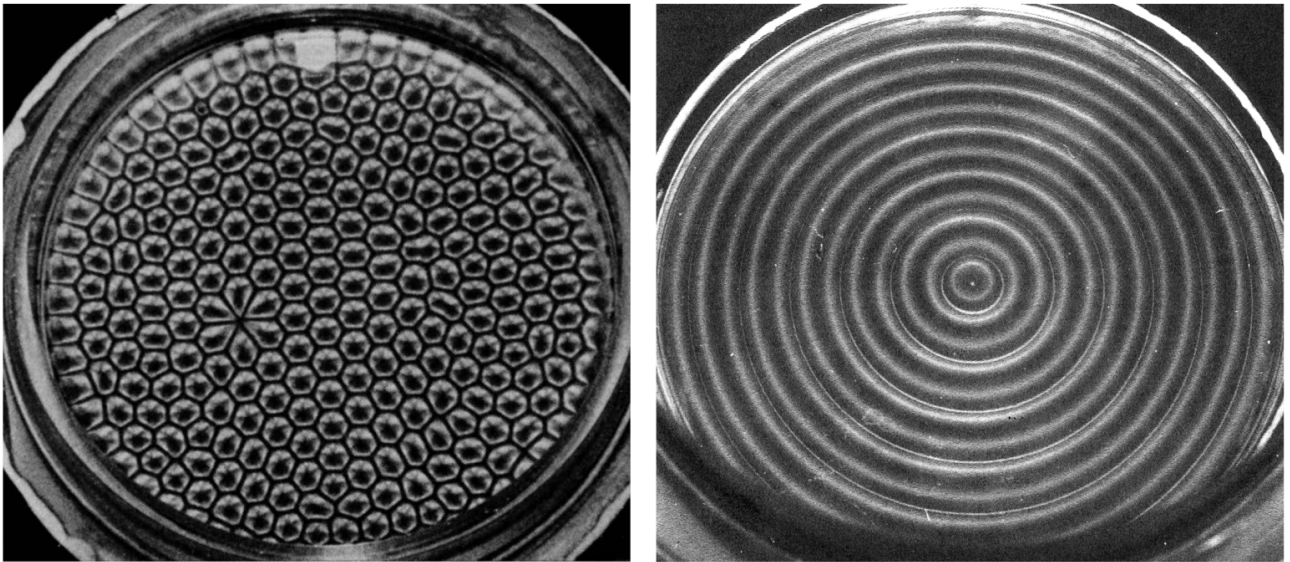


Figure 1.10: (a) Surface tension driven convection leading to the onset of hexagonal Bénard cells in a thin layer of silicone oil, heated from below and cooled by ambient air. A diamond defect appears, likely caused by plate imperfections. (b) Buoyancy driven convection in rigid plates, resulting to concentric convection rolls at 2.9 times the critical Rayleigh number. Both experiments were performed by Koschmieder and Pallas [1974], and the convection patterns were illuminated by aluminum powder, where the dark and bright regions refer to vertical and horizontal motions resepctively. These higher resolution images were taken from [Van Dyke and Van Dyke, 1982].

by Henri Bénard [Bénard, 1901], who observed the formation of hexagonal convection cells above a certain temperature threshold ΔT . These hexagonal patterns are referred to as Bénard cells are illustrated in figure 1.10(a) (adapted from [Koschmieder and Pallas, 1974]). Subsequently, Rayleigh [1916] carried out one of first linear stability analyses of buoyancy-driven convection, predicting the onset of convection at a critical Rayleigh number of $Ra_c = 657.5$. However, Rayleigh's analysis assumed an idealised free-free boundary conditions, which differed from the rigid-free setup of Bénard's experiment. The linear stability analysis for rigid-free configuration was later performed by Jeffreys [1928] yielding a higher critical Rayleigh number of $Ra_c = 1058$. In the rigid-rigid configuration, the critical Rayleigh number increases further to $Ra_c = 1708$ [Pellew and Southwell, 1940]. The Rayleigh number in Bénard's original experiment was found to be 300 to 1500 smaller than Ra_c for the free-free and rigid-free cases [Wesfreid, 2017]. This contradiction, not recognised by Bénard at the time, lies in the significant role of surface tension in thin fluid layers exposed to air, now known as Bénard-Maragoni (BM) convection [Block, 1956, Cloot and Lebon, 1984, Manneville, 2006, Wesfreid, 2017]. In BM convection, fluid motion is primarily driven by surface tension gradients due to variations of temperature, forming hexagonal cells, as in figure 1.10(a). The preference for hexagonal cells in BM convection was later confirmed based on weakly nonlinear stability analysis [Cloot and Lebon, 1984]. As the fluid layer becomes thicker, surface-tension effects diminish and buoyancy-driven convection becomes dominant. Similarly, placing a rigid lid on top of a thin fluid layer suppresses surface-tension effects, also resulting in buoyancy-driven convection. The preferred convection patterns based on weakly nonlinear stability analysis are the two-dimensional parallel rolls,

now referred to as ideal straight rolls (ISRs) [Schlüter et al., 1965, Bodenschatz et al., 2000]. In circular containers, the ISRs conform to the geometry of the boundaries, forming concentric convection rolls illustrated in figure 1.10(b). Interestingly, hexagonal cells have been observed in buoyancy-driven flows of non-Boussinesq fluids [Hoard et al., 1970, Bodenschatz et al., 2000]. In this thesis, I will consider RBC with rigid-rigid boundary conditions with for which the critical Rayleigh number is $Ra_c = 1708$. Notably, the corresponding critical wavelength is $q_c = 3.12/d$ (or $\lambda_c \approx 2d$), suggesting that distance separating the plates, d , dictates the length of a single roll, $l_{roll} = \lambda_c/2 \approx d$.

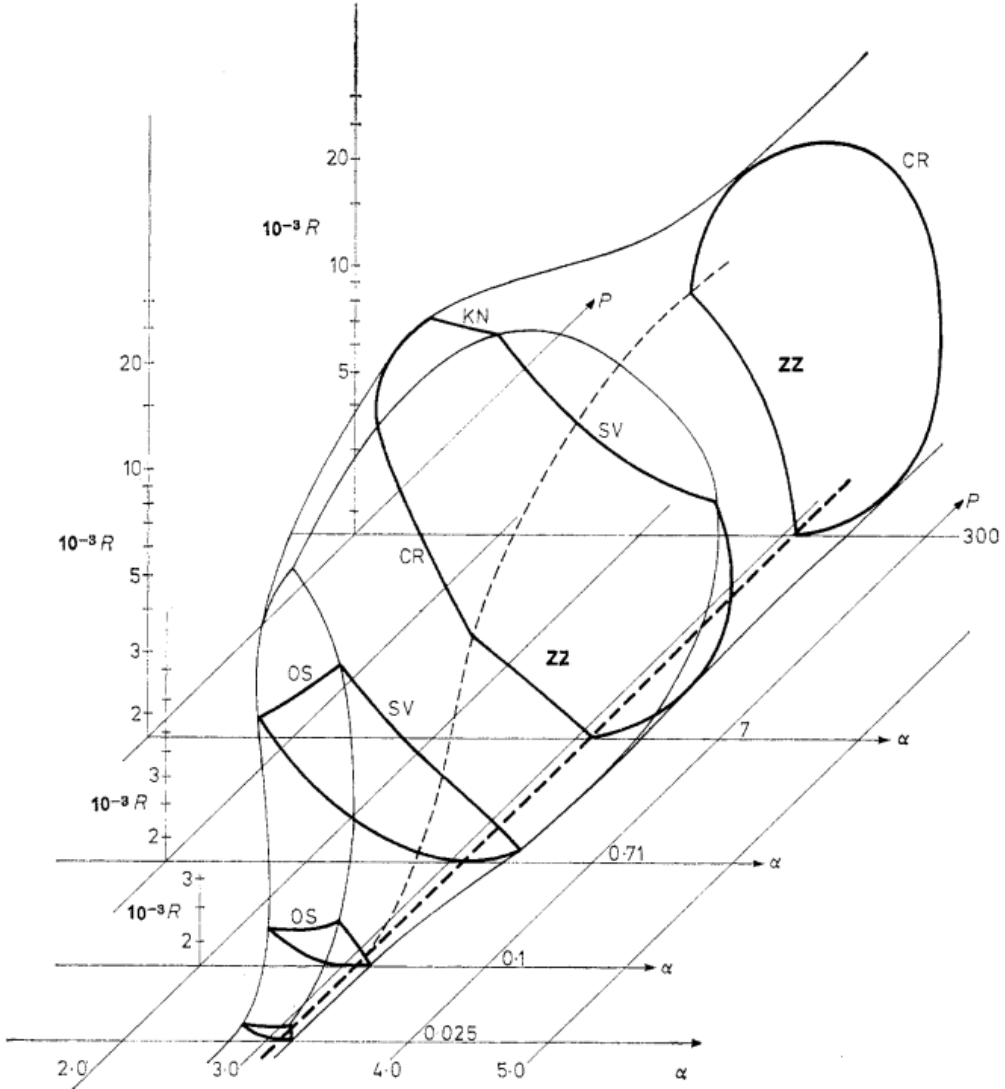


Figure 1.11: The Busse balloon describes the stability boundaries of ISRs in a $\varepsilon - q$ space. For larger wavenumbers, the instability mechanism is described by the skewed-varicose (SV) instability. For smaller wavenumbers, the instability mechanism is described by the Eckhaus instability. For large ε , the instability is described by the onset of oscillatory instability. Busse balloon digitised from [Plapp, 1997] for $Pr \approx 1$.

As mentioned earlier, stationary ISRs near q_c emerge just above Ra_c , based on weakly nonlinear stability analysis. [Eckhaus, 1965, Schlüter et al., 1965]. However, this prediction contradicted by the emergence of time-dependent oscillatory ISRs in experiments [Rossby, 1969, Willis and Deardorff, 1970] at $Ra = 9200$ (or roughly five times Ra_c), where weakly nonlinear stability becomes inapplicable

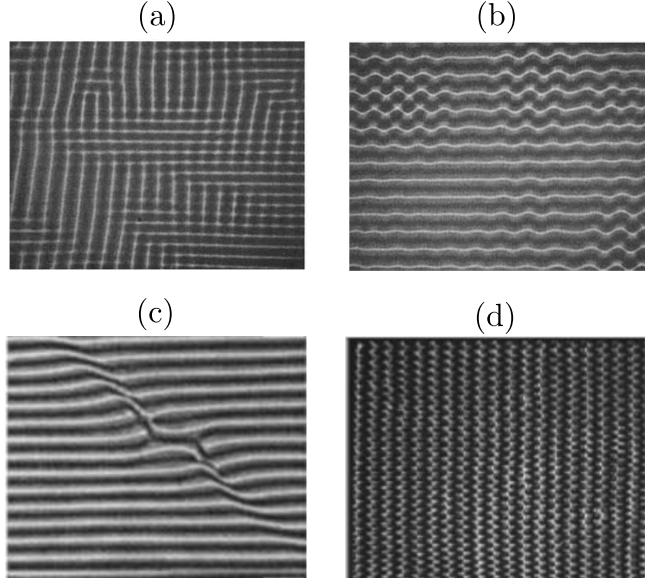


Figure 1.12: ISRs experiencing (a) cross-roll instability at $Ra = 3000, Pr = 100$ and (b) zig-zag instability at $Ra = 3600, Pr = 100$ [Busse and Whitehead, 1971]. (c) Skew-varicosed instability at $Ra = 5568, Pr = 1$ [Plapp, 1997], and (d) oscillatory instability at $Ra = 10384, Pr = 1$ [Cakmur et al., 1997a].

far from threshold. To address this, a direct secondary stability analysis was employed to study the stability of ISRs further from Ra_c , based on Galerkin analysis [Busse, 1972]. The results from the analysis is described by the Busse balloon, which illustrates the stability boundaries of ISRs as a function of Ra and Pr and roll wavenumber, α , shown figure 1.11 [Busse, 1978]. The boundaries of the Busse balloon are described by a range of secondary instabilities, each arising from different physical mechanisms [Busse, 1978]. At large Prandtl numbers, $Pr = O(10^2)$, the zig-zag (ZZ) and cross-roll (CR) instabilities delimits the balloon for small and large roll wavenumbers. The zig-zag instabilities cause zig-zag undulations while the CR instabilities generates rolls orthogonal to the underlying ISR structure, effectively increasing or decreasing the roll wavenumber respectively [Busse and Whitehead, 1971]. Examples of these instabilities at $Pr = 100$ are illustrated in figure 1.12(a,b).

At moderate Prandtl numbers, $Pr = O(1)$, the Busee balloon is bounded by the skewed varicosed (SV) for high roll wavenumbers and the oscillatory (OS) instability at large Ra . The skewed-varicosed (SV) instability leads to roll-pinchig where pinched rolls merged into a single roll, reducing roll wavenumber while the oscillatory instability leads to the onset of an oscillatory ISRs. Examples of the respective instabilities at $Pr = 1$ are shown in figure 1.12(c,d). At higher wavenumbers, the skewed varicose (SV) instability becomes relevant at intermediate Prandlt numbers, characterised by roll pinching and merging that effectively reduces the roll wavenumber. Finally, the Eckhaus instability (not shown), related to the symmetry of the system, appears close to the Ra_c , leading a disturbance parallel to the underlying rolls which either creates or destroy rolls such that the resultant roll wavenumber adheres to the stability boundaries [Lowe and Gollub, 1985]. Near $Pr = 1$, the Eckhaus instability coincides with the crossroll instability (figure 6 from Bodenschatz et al. [2000], adapted from Plapp [1997].) In this thesis, we focus on fluids with $Pr = 1$, where secondary instabilities such as skewed-varicose, Eckhaus and cross-roll instabilities typically arise. While the stability boundaries of the

Busse balloon have been experimentally verified [Busse and Whitehead, 1971, Croquette, 1989a, Plapp, 1997], accurately predicting the wavenumber of ideal straight rolls (ISRs) remain difficult due to hysteresis. As Ra is continuously increases, ISRs with wavenumbers outside the Busse Balloon undergo the secondary instabilities (described above) that drive their wavenumbers back to the stable boundaries. The hysteretic behaviour highlights that the roll wavenumber of the ISRs is strongly dependent on the system's history [Bodenschatz et al., 2000].

It is worth noting that the ISRs are the exception rather than the rule in RBC [Croquette, 1989b]. A range of non-ISR states, such as squares, travelling or stationary target patterns, giant rotating spirals, and oscillatory convection, have been observed over the years [Le Gal et al., 1985, Croquette, 1989a, Plapp, 1997, Hof et al., 1999, Rüdiger and Feudel, 2000, Borońska and Tuckerman, 2010a,b]. For example, Hof et al. [1999] identified eight stationary and two oscillatory state in cylindrical RBC with small aspect ratios at the same Rayleigh number. These results were later verified in numerical simulations and bifurcation analysis, reveal up to twelve stable branches near the onset ($Ra \leq 2500$) and the potential for hundreds more as Ra increases [Ma et al., 2006, Borońska and Tuckerman, 2010a,b].

In larger domains ($\Gamma \geq 28$), giant rotating spirals were found and have been investigated [Plapp and Bodenschatz, 1996, Plapp et al., 1998]. Experimental and numerical studies of RBC with varying sidewall boundary conditions (i.e. thermally insulating, conducting and no-slip) [Tuckerman and Barkley, 1988, Siggers, 2003, Paul et al., 2003, Bouillé et al., 2022], non-Boussinesq convection [Bodenschatz et al., 1992], and rotational effects [Hu et al., 1997] were investigated, where multiple states were also reported. In inclined RBC, Reetz and Schneider [2020], Reetz et al. [2020] identified up to sixteen stable and unstable invariant states, along with heteroclinic orbits connecting them. These findings indicate that RBC support a rich variety of coexisting stable states beyond ISRs, resulting to a system with multiple stable states above the critical Rayleigh number. To complicate matters further, RBC also exhibits spatiotemporal chaotic states.

In the late 1990s, convection rolls exhibiting spatio-temporal chaotic behaviour known as spiral defect chaos (SDC) were observed within the same stability boundaries where ISRs were expected [Morris et al., 1993, Hu et al., 1993, Decker et al., 1994, Hu et al., 1995, Morris et al., 1996, Cakmur et al., 1997a, Ahlers, Egolf et al., 1998, 2000, Chiam et al., 2003, Vitral et al., 2020]. Notably, ISRs emerge with carefully prepared initial conditions while uncontrolled initial conditions lead to SDC. It is now well established that SDC exists as intrinsic attractor of RBC, independent of sidewall conditions Morris et al. [1996], forming a bistable system with ISRs [Cakmur et al., 1997a] across a range of Ra at $Pr = 1$ illustrated in figure 1.13. However, this bistability appears to be Prandtl number dependent. At $Pr = 4$, the SDC appears to be transient decaying towards ISRs over long periods [Bajaj et al., 1997]. SDC has also been replicated in numerical simulations using two-dimensional Swift-Hohenberg equations [Swift and Hohenberg, 1977, Xi et al., 1993, Xi and Gunton, 1995, Schmitz et al., 2002, Karimi et al., 2011]. The critical Rayleigh number for the onset of SDC, Ra_s , depends on the domain's aspect ratio, and Prandtl number [Hu et al., 1995, Bajaj et al., 1997, Cakmur et al., 1997b, Bodenschatz et al., 2000]. SDC has been primarily reported in large aspect ratio domains ($\Gamma \gtrsim 20$), suggesting a minimal domain size for SDC to occur [Bodenschatz et al.,

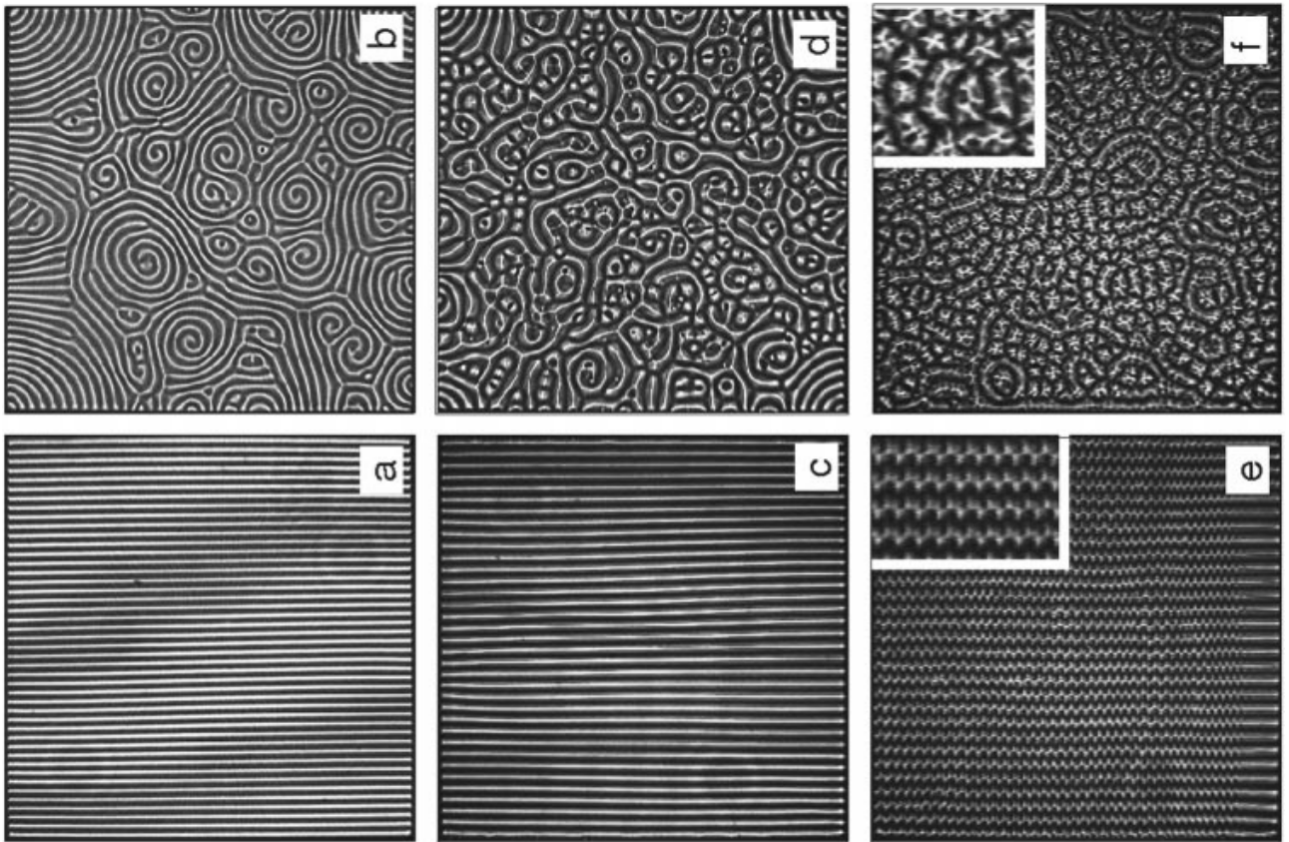


Figure 1.13: The coexistence of spiral defect chaos (SDC, top row) and ideal straight rolls (ISRs, bottom row) at (a,b) $Ra = 3279$, (c,d) $Ra = 6832$ and (e,f) $Ra = 10384$. The domain size is $\Gamma = 50$ and $Pr = 1$, adapted from Cakmur et al. [1997a].

2000]. Furthermore, the leading Lyapunov exponents of SDC decreases as Γ [Egolf et al., 2000, Paul et al., 2007]. To better characterise SDC, several studies have investigated its spatial-temporal properties, such as the averaged roll-curvature Hu et al. [1995], probability distribution of spirals Ecke et al. [1995], Liu and Ahlers [1996] and correlation length-/time-scales [Morris et al., 1993, 1996, Cakmur et al., 1997b]. Specifically, the correlation length-scales were found to grow exponentially with [Morris et al., 1993, 1996, Cakmur et al., 1997b], suggesting that transition from ISRs to SDC resembles a phase transition. Similar spatiotemporal chaotic behaviour has been observed in other pattern-formation systems, including rotating RBC Hu et al. [1997], dielectric barrier discharge Dong et al. [2005] and advection diffusion reaction systems Affan and Friedrich [2014].

1.4 Rayleigh-Bénard Poiseuille (RBP) flows

This section describes the development of Rayleigh-Bénard Poiseuille (RBP) flows, integrating key findings from both Rayleigh-Bénard convection (RBC) and plane Poiseuille flow (PPF) systems discussed earlier. The neutral stability curves in the Rayleigh-Bénard Poiseuille (RBP) comprising of both plane Poisueuille flow (PPF) and Rayleigh-Béanrd convection (RBC) systems, are bounded by the onset of Tollmien-Schlichting waves at $Re_c = 5772.22$ [Orszag, 1971], and by the onset of convection

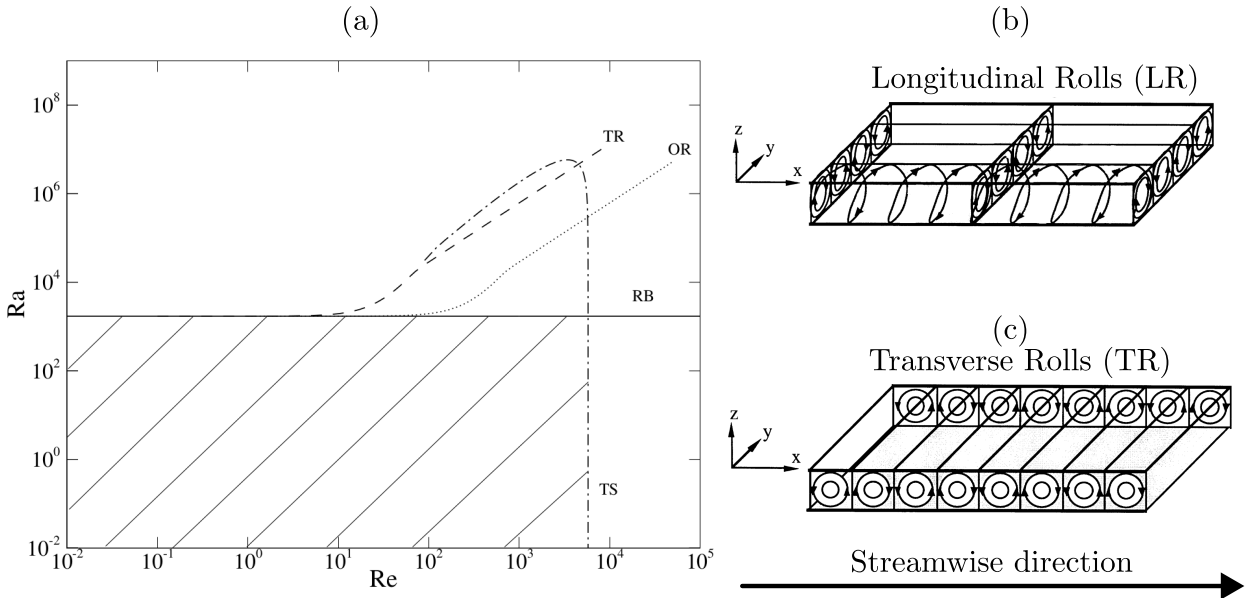


Figure 1.14: (a) Neutral stability curves of longitudinal rolls (LR), oblique rolls (OR), transverse rolls (TR) and Tollmien-Schlichting (TS) waves, adapted from John Soundar Jerome et al. [2012]. The shaded area refers to damped perturbations. Sketch of (b) longitudinal and (c) transverse rolls, adapted from Kelly [1994].

rolls at $Ra_c = 1708$ [Pellew and Southwell, 1940], respectively. In RBP systems, the imposed mean Poiseuille flow in the RBP system breaks the rotational symmetry of the convection rolls, categorising them based on their orientation to the mean flow direction, namely: longitudinal ($\alpha = 0, \beta \neq 0$), transverse ($\alpha \neq 0, \beta = 0$) and oblique rolls ($\alpha \neq 0, \beta \neq 0$). These primary instabilities were first investigated by Gage and Reid [1968] in an infinitely extended layer. For longitudinal rolls, the linearised system reduces to the classical RBC problem. Thus, the critical Rayleigh number remains unchanged at $Ra_{\parallel} = Ra_c = 1708.8$ with a critical wavenumber, $\alpha_{\parallel} = \alpha_c = 3.13$, independent of Reynolds number Re and Prandtl number Pr [Pellew and Southwell, 1940, Kelly, 1994]. In contrast, the critical Rayleigh number for the onset of transverse rolls increases with Re , dependent on Pr [Gage and Reid, 1968, Müller et al., 1992, Nicolas et al., 1997]. The critical Rayleigh number for the onset of obliqued rolls can derived using by applying a Squire transformation [Squire, 1933] to transverse roll system. For a given Ra , the corresponding critical Re for the onset of oblique rolls is higher than that for transverse rolls [Gage and Reid, 1968]. The neutral stability curves for the three different rolls are illustrated in figure 1.14.

Experimental studies in channels with large transverse aspect ratios (i.e. span-to-depth) showed the onset of longitudinal rolls [Akiyama et al., 1971, Ostrach and Kamotani, 1975, Fukui et al., 1983], while transverse rolls are more prevalent in narrower channels [Luijckx et al., 1981, Ouazzani et al., 1989, 1990]. Linear stability analysis of longitudinal rolls for finite channels confirms that Ra_{\parallel} remains fairly independent for transverse aspect ratios greater than five, and increases quickly below that. Hence, for small Re , critical Rayleigh number of transverse rolls is smaller than that of longitudinal rolls, $Ra_{\perp} < Ra_{\parallel}$, giving rise to transverse rolls [Nicolas et al., 2000]. However, temporal linear stability analysis could not explain the observations by Ouazzani et al. [1990], where the laminar Poiseuille

flow persisted in the same parameter space where transverse rolls were expected. This discrepancy was resolved by Müller et al. [1992], who showed that transverse rolls may be convectively or absolutely unstable, with the transition boundary aligning with the experimental data. Later, Carrière and Monkewitz [1999] showed that demonstrated that longitudinal rolls are always convectively unstable. Nonmodal stability analysis of subcritical RBP by John Soundar Jerome et al. [2012] revealed that the optimal transient growth is primarily dominated by streamwise rollers similar to those of PPF [Reddy and Henningson, 1993], with a spanwise wavenumber of $\beta_{opt} \approx 2.05$. The maximum amplification factor, G_{max} increases modestly with Ra , and the critical wavenumber approaches α_{\parallel} , indicative of longitudinal rolls. For $Re > 0$ in infinite domains, longitudinal rolls emerge as the dominant primary instability [Gage and Reid, 1968]. Their secondary stability was analysed by [Clever and Busse, 1991], who identified a time-dependent, wavy instability near $Re \sim 100$, giving rise to tertiary solutions in the form of wavy rolls. These wavy rolls have been observed experimentally and were found to be convectively unstable [Pabiou et al., 2003, 2005, Nicolas et al., 2010]. Clever and Busse [1991] also hypothesised that the wavy rolls are less efficient at transporting heating than longitudinal rolls for the same Ra , which was later confirmed numerically [Nicolas et al., 2012]. The influence of finite transverse aspect ratios on the onset of wavy rolls have also been studied [Xin et al., 2006, Nicolas et al., 2010], where the critical Ra was found to be approximately 1.5 times higher than in infinite domains Clever and Busse [1991]. Furthermore, the effect of external excitation has been explored, showing that increased excitation amplitude can reduce the development length required for wavy roll formation [Nicolas et al., 2010, 2012]. In the turbulent regime, shear driven turbulence has been shown to enhance heat transport in RBP flows [Scagliarini et al., 2014, 2015, Pirozzoli et al., 2017]. Extensions of the RBP configuration, such as flows over wavy walls or with sinusoidal thermal forcing have been investigated, potentially offering a reduction in drag and enhancing heat transport [Hossain et al., 2012, Hossain and Floryan, 2016, 2020]. For a comprehensive overview of RBP flows, the reader is referred to the reviews by Kelly [1994] and Nicolas [2002].

1.4.1 Thesis Outline

In this thesis, I am particularly focused on the transition behaviour of fluid flow driven by shear and buoyancy, addressing questions related to the onset of instabilities due to shear and buoyancy, and the (possible) competitive between shear and buoyancy driven instabilities. I would like to preface that while this thesis is dealing with onset of instabilities, it does not clearly indicate that the onset of such instabilities necessarily lead to turbulence, hence, for terminology sake, we shall be looking into transitional regimes where the fluid neither laminar nor turbulent. The main motivations are two-folds, both from an academic and applied point-of-view. Within academia, the onset and transition to turbulence in Rayleigh-Bénard Poiseuille flows remains poorly understood. Whilst there had been significant progress in our understanding of transition to turbulence in independent setups, Rayleigh-Bénard convection and plane Poiseuille flows, their combined effects are not known. The thesis is structured into the following, Chapter 1 is the introduction with literature review, chapter 2 methodology associated with the spectral/ hp -element method, chapter 3 with results related to the the Rayleigh and Reynolds number sweep, chapter 4 with a specific focus on the bistability between spiral defect chaos

and ideal straight rolls and finally chapter 5 with concluding remarks.

1. Academic motivation - flow structures, statistics, transition.
2. Application motivation - shear, heat transfer. Chip cooling, thin-film fabrication and atmospheric boundary layer.

We seek to investigate the influence of unstable stratification quantified by Rayleigh number Ra , on the behaviour turbulent-laminar bands. The onset of convection occurs at a critical Rayleigh number of $Ra_c > 1708$, in the form of a pair of convection rolls. When aligned in the streamwise direction, the convection rolls are seemingly analogous to a pair of counter-rotating vortices, an optimal initial condition for transient growth. Our investigation naturally answers a few questions related to turbulent-laminar bands. For example, does the onset of turbulent-laminar bands, Re_{cr} decrease with increasing Ra ? Do Ra -effects influence the structure of turbulent-laminar bands i.e band angle/width?

The answers to our research will have important implications Rayleigh-Bénard Poiseuille flows, ubiquitous in atmospheric, geophysical and engineering flows.

Bibliography

Clouds streets and comma clouds near svalbard. <https://earthobservatory.nasa.gov/images/87749/clouds-streets-and-comma-clouds-near-svalbard>.

H. Affan and R. Friedrich. Spiral defect chaos in an advection-reaction-diffusion system. *Physical Review E*, 89(6):062920, June 2014. ISSN 1539-3755, 1550-2376. doi: 10.1103/PhysRevE.89.062920. URL <https://link.aps.org/doi/10.1103/PhysRevE.89.062920>.

Guenter Ahlers. Experiments on spatio-temporal chaos.

Mitsunobu Akiyama, Guang-Jyh Hwang, and KC Cheng. Experiments on the onset of longitudinal vortices in laminar forced convection between horizontal plates. 1971. ISSN 0022-1481.

Edward Anderson, Zhaojun Bai, Christian Bischof, L Susan Blackford, James Demmel, Jack Dongarra, Jeremy Du Croz, Anne Greenbaum, Sven Hammarling, and Alan McKenney. *LAPACK users' guide*. SIAM, 1999. ISBN 0-89871-447-8.

Walter Edwin Arnoldi. The principle of minimized iterations in the solution of the matrix eigenvalue problem. *Quarterly of applied mathematics*, 9(1):17–29, 1951. ISSN 0033-569X.

Kerstin Avila, David Moxey, Alberto De Lozar, Marc Avila, Dwight Barkley, and Björn Hof. The Onset of Turbulence in Pipe Flow. *Science*, 333(6039):192–196, July 2011. ISSN 0036-8075, 1095-9203. doi: 10.1126/science.1203223. URL <https://www.science.org/doi/10.1126/science.1203223>.

Marc Avila, Ashley P. Willis, and Björn Hof. On the transient nature of localized pipe flow turbulence. *Journal of Fluid Mechanics*, 646:127–136, March 2010. ISSN 0022-1120, 1469-7645. doi: 10.1017/S0022112009993296. URL https://www.cambridge.org/core/product/identifier/S0022112009993296/type/journal_article.

Marc Avila, Dwight Barkley, and Björn Hof. Transition to Turbulence in Pipe Flow. *Annual Review of Fluid Mechanics*, 55(1):575–602, January 2023. ISSN 0066-4189, 1545-4479. doi: 10.1146/annurev-fluid-120720-025957. URL <https://www.annualreviews.org/doi/10.1146/annurev-fluid-120720-025957>.

Kapil M. S. Bajaj, David S. Cannell, and Guenter Ahlers. Competition between spiral-defect chaos and rolls in Rayleigh-Bénard convection. *Physical Review E*, 55(5):R4869–R4872, May 1997. ISSN

1063-651X, 1095-3787. doi: 10.1103/PhysRevE.55.R4869. URL <https://link.aps.org/doi/10.1103/PhysRevE.55.R4869>.

D. Barkley, H. M. Blackburn, and S. J. Sherwin. Direct optimal growth analysis for timesteppers. *International Journal for Numerical Methods in Fluids*, 57(9):1435–1458, July 2008. ISSN 0271-2091, 1097-0363. doi: 10.1002/fld.1824. URL <https://onlinelibrary.wiley.com/doi/10.1002/fld.1824>.

Dwight Barkley and Laurette S. Tuckerman. Computational Study of Turbulent Laminar Patterns in Couette Flow. *Physical Review Letters*, 94(1):014502, January 2005. doi: 10.1103/PhysRevLett.94.014502. URL <https://link.aps.org/doi/10.1103/PhysRevLett.94.014502>. Publisher: American Physical Society.

Dwight Barkley and Laurette S Tuckerman. Mean flow of turbulent–laminar patterns in plane Couette flow. *Journal of Fluid Mechanics*, 576:109–137, 2007. ISSN 1469-7645. Publisher: Cambridge University Press.

Myron J. Block. Surface Tension as the Cause of Bénard Cells and Surface Deformation in a Liquid Film. *Nature*, 178(4534):650–651, September 1956. ISSN 0028-0836, 1476-4687. doi: 10.1038/178650a0. URL <https://www.nature.com/articles/178650a0>.

Eberhard Bodenschatz, David S. Cannell, John R. De Bruyn, Robert Ecke, Yu-Chou Hu, Kristina Lerman, and Guenter Ahlers. Experiments on three systems with non-variational aspects. *Physica D: Nonlinear Phenomena*, 61(1-4):77–93, December 1992. ISSN 01672789. doi: 10.1016/0167-2789(92)90150-L. URL <https://linkinghub.elsevier.com/retrieve/pii/016727899290150L>.

Eberhard Bodenschatz, Werner Pesch, and Guenter Ahlers. Recent Developments in Rayleigh-Bénard Convection. *Annual Review of Fluid Mechanics*, 32(1):709–778, January 2000. ISSN 0066-4189, 1545-4479. doi: 10.1146/annurev.fluid.32.1.709. URL <https://www.annualreviews.org/doi/10.1146/annurev.fluid.32.1.709>.

Katarzyna Borońska and Laurette S. Tuckerman. Extreme multiplicity in cylindrical Rayleigh-Bénard convection. I. Time dependence and oscillations. *Physical Review E*, 81(3):036320, March 2010a. ISSN 1539-3755, 1550-2376. doi: 10.1103/PhysRevE.81.036320. URL <https://link.aps.org/doi/10.1103/PhysRevE.81.036320>.

Katarzyna Borońska and Laurette S. Tuckerman. Extreme multiplicity in cylindrical Rayleigh-Bénard convection. II. Bifurcation diagram and symmetry classification. *Physical Review E*, 81(3):036321, March 2010b. ISSN 1539-3755, 1550-2376. doi: 10.1103/PhysRevE.81.036321. URL <https://link.aps.org/doi/10.1103/PhysRevE.81.036321>.

S Bottin, F Daviaud, P Manneville, and O Dauchot. Discontinuous transition to spatiotemporal intermittency in plane Couette flow. *Europhysics Letters (EPL)*, 43(2):171–176, July 1998. ISSN

0295-5075, 1286-4854. doi: 10.1209/epl/i1998-00336-3. URL <https://iopscience.iop.org/article/10.1209/epl/i1998-00336-3>.

N. Boullié, V. Dallas, and P. E. Farrell. Bifurcation analysis of two-dimensional Rayleigh-Bénard convection using deflation. *Physical Review E*, 105(5):055106, May 2022. ISSN 2470-0045, 2470-0053. doi: 10.1103/PhysRevE.105.055106. URL <https://link.aps.org/doi/10.1103/PhysRevE.105.055106>.

F. H. Busse. The oscillatory instability of convection rolls in a low Prandtl number fluid. *Journal of Fluid Mechanics*, 52(1):97–112, March 1972. ISSN 0022-1120, 1469-7645. doi: 10.1017/S0022112072002988. URL https://www.cambridge.org/core/product/identifier/S0022112072002988/type/journal_article.

F H Busse. Non-linear properties of thermal convection. *Reports on Progress in Physics*, 41(12):1929–1967, December 1978. ISSN 0034-4885, 1361-6633. doi: 10.1088/0034-4885/41/12/003. URL <https://iopscience.iop.org/article/10.1088/0034-4885/41/12/003>.

F. H. Busse and J. A. Whitehead. Instabilities of convection rolls in a high Prandtl number fluid. *Journal of Fluid Mechanics*, 47(2):305–320, May 1971. ISSN 0022-1120, 1469-7645. doi: 10.1017/S0022112071001071. URL https://www.cambridge.org/core/product/identifier/S0022112071001071/type/journal_article.

Kathryn M. Butler and Brian F. Farrell. Three-dimensional optimal perturbations in viscous shear flow. *Physics of Fluids A: Fluid Dynamics*, 4(8):1637–1650, August 1992. ISSN 0899-8213. doi: 10.1063/1.858386. URL <https://pubs.aip.org/pof/article/4/8/1637/402702/Three-dimensional-optimal-perturbations-in-viscous>.

Henri Bénard. Les tourbillons cellulaires dans une nappe liquide. - Méthodes optiques d’observation et d’enregistrement. *Journal de Physique Théorique et Appliquée*, 10(1):254–266, 1901. ISSN 0368-3893. doi: 10.1051/jphystab:0190100100025400. URL <http://www.edpsciences.org/10.1051/jphystab:0190100100025400>.

Reha V. Cakmur, David A. Egolf, Brendan B. Plapp, and Eberhard Bodenschatz. Bistability and Competition of Spatiotemporal Chaotic and Fixed Point Attractors in Rayleigh-Bénard Convection. *Physical Review Letters*, 79(10):1853–1856, September 1997a. ISSN 0031-9007, 1079-7114. doi: 10.1103/PhysRevLett.79.1853. URL <https://link.aps.org/doi/10.1103/PhysRevLett.79.1853>.

Reha V. Cakmur, David A. Egolf, Brendan B. Plapp, and Eberhard Bodenschatz. Transition from Spatiotemporal Chaos to Ideal Straight Rolls in Rayleigh-Benard Convection, February 1997b. URL <http://arxiv.org/abs/patt-sol/9702003>. arXiv:patt-sol/9702003.

Philippe Carrière and Peter A. Monkewitz. Convective versus absolute instability in mixed Rayleigh-Bénard-Poiseuille convection. *Journal of Fluid Mechanics*, 384:243–262, April 1999. ISSN 0022-1120, 1469-7645. doi: 10.1017/

S0022112098004145. URL https://www.cambridge.org/core/product/identifier/S0022112098004145/type/journal_article.

Subrahmanyam Chandrasekhar. The stability of spiral flow between rotating cylinders. *Philosophical Transactions of the Royal Society of London. Series A, Mathematical and Physical Sciences*, 263 (1135):57–91, May 1968. ISSN 0080-4614, 2054-0272. doi: 10.1098/rsta.1968.0006. URL <https://royalsocietypublishing.org/doi/10.1098/rsta.1968.0006>.

K.-H. Chiam, M. R. Paul, M. C. Cross, and H. S. Greenside. Mean flow and spiral defect chaos in Rayleigh-Bénard convection. *Physical Review E*, 67(5):056206, May 2003. ISSN 1063-651X, 1095-3787. doi: 10.1103/PhysRevE.67.056206. URL <https://link.aps.org/doi/10.1103/PhysRevE.67.056206>.

Alexandre Joel Chorin. A numerical method for solving incompressible viscous flow problems. *Journal of Computational Physics*, 2(1):12–26, August 1967. ISSN 00219991. doi: 10.1016/0021-9991(67)90037-X. URL <https://linkinghub.elsevier.com/retrieve/pii/002199916790037X>.

Douglas C. Chu and George Em Karniadakis. A direct numerical simulation of laminar and turbulent flow over riblet-mounted surfaces. *Journal of Fluid Mechanics*, 250:1–42, May 1993. ISSN 0022-1120, 1469-7645. doi: 10.1017/S0022112093001363. URL https://www.cambridge.org/core/product/identifier/S0022112093001363/type/journal_article.

R. M. Clever and F. H. Busse. Instabilities of longitudinal rolls in the presence of Poiseuille flow. *Journal of Fluid Mechanics*, 229(-1):517, August 1991. ISSN 0022-1120, 1469-7645. doi: 10.1017/S0022112091003142. URL http://www.journals.cambridge.org/abstract_S0022112091003142.

A. Cloot and G. Lebon. A nonlinear stability analysis of the Bénard–Marangoni problem. *Journal of Fluid Mechanics*, 145(-1):447, August 1984. ISSN 0022-1120, 1469-7645. doi: 10.1017/S0022112084003013. URL http://www.journals.cambridge.org/abstract_S0022112084003013.

Vincent Croquette. Convective pattern dynamics at low Prandtl number: Part I. *Contemporary Physics*, 30(2):113–133, March 1989a. ISSN 0010-7514, 1366-5812. doi: 10.1080/00107518908225511. URL <http://www.tandfonline.com/doi/abs/10.1080/00107518908225511>.

Vincent Croquette. Convective pattern dynamics at low Prandtl number: Part II. *Contemporary Physics*, 30(3):153–171, May 1989b. ISSN 0010-7514, 1366-5812. doi: 10.1080/00107518908222594. URL <http://www.tandfonline.com/doi/abs/10.1080/00107518908222594>.

P Cvitanović and J F Gibson. Geometry of the turbulence in wall-bounded shear flows: periodic orbits. *Physica Scripta*, T142:014007, December 2010. ISSN 0031-8949, 1402-4896. doi:

10.1088/0031-8949/2010/T142/014007. URL <https://iopscience.iop.org/article/10.1088/0031-8949/2010/T142/014007>.

S. J. Davies and C. M. White. An experimental study of the flow of water in pipes of rectangular section. *Proceedings of the Royal Society of London. Series A, Containing Papers of a Mathematical and Physical Character*, 119(781):92–107, May 1928. ISSN 0950-1207, 2053-9150. doi: 10.1098/rspa.1928.0086. URL <https://royalsocietypublishing.org/doi/10.1098/rspa.1928.0086>.

R. B. Dean. Reynolds Number Dependence of Skin Friction and Other Bulk Flow Variables in Two-Dimensional Rectangular Duct Flow. *Journal of Fluids Engineering*, 100(2):215–223, June 1978. ISSN 0098-2202, 1528-901X. doi: 10.1115/1.3448633. URL <https://asmedigitalcollection.asme.org/fluidsengineering/article/100/2/215/409704/Reynolds-Number-Dependence-of-Skin-Friction-and>.

W. Decker, W. Pesch, and A. Weber. Spiral defect chaos in Rayleigh-Bénard convection. *Physical Review Letters*, 73(5):648–651, August 1994. ISSN 0031-9007. doi: 10.1103/PhysRevLett.73.648. URL <https://link.aps.org/doi/10.1103/PhysRevLett.73.648>.

Juan C. Del Álamo and Javier Jiménez. Linear energy amplification in turbulent channels. *Journal of Fluid Mechanics*, 559:205, July 2006. ISSN 0022-1120, 1469-7645. doi: 10.1017/S0022112006000607. URL http://www.journals.cambridge.org/abstract_S0022112006000607.

Lifang Dong, Fucheng Liu, Shuhua Liu, Yafeng He, and Weili Fan. Observation of spiral pattern and spiral defect chaos in dielectric barrier discharge in argon/air at atmospheric pressure. *Physical Review E*, 72(4):046215, October 2005. ISSN 1539-3755, 1550-2376. doi: 10.1103/PhysRevE.72.046215. URL <https://link.aps.org/doi/10.1103/PhysRevE.72.046215>.

Y. Duguet, A. P. Willis, and R. R. Kerswell. Transition in pipe flow: the saddle structure on the boundary of turbulence. *Journal of Fluid Mechanics*, 613:255–274, October 2008. ISSN 0022-1120, 1469-7645. doi: 10.1017/S0022112008003248. URL https://www.cambridge.org/core/product/identifier/S0022112008003248/type/journal_article.

Y. Duguet, P. Schlatter, and D. S. Henningson. Formation of turbulent patterns near the onset of transition in plane Couette flow. *Journal of Fluid Mechanics*, 650:119–129, May 2010. ISSN 0022-1120, 1469-7645. doi: 10.1017/S0022112010000297. URL https://www.cambridge.org/core/product/identifier/S0022112010000297/type/journal_article.

Robert E. Ecke, Yuchou Hu, Ronnie Mainieri, and Guenter Ahlers. Excitation of Spirals and Chiral Symmetry Breaking in Rayleigh-Bénard Convection. *Science*, 269(5231):1704–1707, September 1995. ISSN 0036-8075, 1095-9203. doi: 10.1126/science.269.5231.1704. URL <https://www.science.org/doi/10.1126/science.269.5231.1704>.

Wiktor Eckhaus. *Studies in Non-Linear Stability Theory*, volume 6 of *Springer Tracts in Natural Philosophy*. Springer Berlin Heidelberg, Berlin, Heidelberg, 1965. ISBN 978-3-642-88319-4

978-3-642-88317-0. doi: 10.1007/978-3-642-88317-0. URL <http://link.springer.com/10.1007/978-3-642-88317-0>.

David A. Egolf, Ilarion V. Melnikov, and Eberhard Bodenschatz. Importance of Local Pattern Properties in Spiral Defect Chaos. *Physical Review Letters*, 80(15):3228–3231, April 1998. ISSN 0031-9007, 1079-7114. doi: 10.1103/PhysRevLett.80.3228. URL <https://link.aps.org/doi/10.1103/PhysRevLett.80.3228>.

David A. Egolf, Ilarion V. Melnikov, Werner Pesch, and Robert E. Ecke. Mechanisms of extensive spatiotemporal chaos in Rayleigh–Bénard convection. *Nature*, 404(6779):733–736, April 2000. ISSN 0028-0836, 1476-4687. doi: 10.1038/35008013. URL <https://www.nature.com/articles/35008013>.

T. Ellingsen and E. Palm. Stability of linear flow. *The Physics of Fluids*, 18(4):487–488, April 1975. ISSN 0031-9171. doi: 10.1063/1.861156. URL <https://pubs.aip.org/pfl/article/18/4/487/459138/Stability-of-linear-flow>.

Greg Evans and Ralph Greif. Unsteady three-dimensional mixed convection in a heated horizontal channel with applications to chemical vapor deposition. *International Journal of Heat and Mass Transfer*, 34(8):2039–2051, August 1991. ISSN 00179310. doi: 10.1016/0017-9310(91)90215-Z. URL <https://linkinghub.elsevier.com/retrieve/pii/001793109190215Z>.

Holger Faisst and Bruno Eckhardt. Traveling Waves in Pipe Flow. *Physical Review Letters*, 91(22):224502, November 2003. ISSN 0031-9007, 1079-7114. doi: 10.1103/PhysRevLett.91.224502. URL <https://link.aps.org/doi/10.1103/PhysRevLett.91.224502>.

Holger Faisst and Bruno Eckhardt. Sensitive dependence on initial conditions in transition to turbulence in pipe flow. *Journal of Fluid Mechanics*, 504:343–352, April 2004. ISSN 0022-1120, 1469-7645. doi: 10.1017/S0022112004008134. URL http://www.journals.cambridge.org/abstract_S0022112004008134.

Brian F. Farrell. Optimal excitation of perturbations in viscous shear flow. *The Physics of Fluids*, 31(8):2093–2102, August 1988. ISSN 0031-9171. doi: 10.1063/1.866609. URL <https://pubs.aip.org/pfl/article/31/8/2093/966463/Optimal-excitation-of-perturbations-in-viscous>.

Mitchell J Feigenbaum. The universal metric properties of nonlinear transformations. *Journal of Statistical Physics*, 21:669–706, 1979. ISSN 0022-4715. Publisher: Springer.

Ciprian Foias, George R Sell, and Roger Temam. Inertial manifolds for nonlinear evolutionary equations. *Journal of Differential Equations*, 73(2):309–353, June 1988. ISSN 00220396. doi: 10.1016/0022-0396(88)90110-6. URL <https://linkinghub.elsevier.com/retrieve/pii/0022039688901106>.

Keisuke Fukui, Masamoto Nakajima, and Hiromasa Ueda. The longitudinal vortex and its effects on the transport processes in combined free and forced laminar convection between horizontal and inclined parallel plates. *International Journal of Heat and Mass Transfer*, 26(1):109–120, January 1983. ISSN 00179310. doi: 10.1016/S0017-9310(83)80013-1. URL <https://linkinghub.elsevier.com/retrieve/pii/S0017931083800131>.

K. S. Gage and W. H. Reid. The stability of thermally stratified plane Poiseuille flow. *Journal of Fluid Mechanics*, 33(1):21–32, July 1968. ISSN 0022-1120, 1469-7645. doi: 10.1017/S0022112068002326. URL https://www.cambridge.org/core/product/identifier/S0022112068002326/type/journal_article.

J. F. Gibson, J. Halcrow, and P. Cvitanović. Visualizing the geometry of state space in plane Couette flow. *Journal of Fluid Mechanics*, 611:107–130, September 2008. ISSN 0022-1120, 1469-7645. doi: 10.1017/S002211200800267X. URL https://www.cambridge.org/core/product/identifier/S002211200800267X/type/journal_article.

J. F. Gibson, J. Halcrow, and P. Cvitanović. Equilibrium and travelling-wave solutions of plane Couette flow. *Journal of Fluid Mechanics*, 638:243–266, November 2009. ISSN 0022-1120, 1469-7645. doi: 10.1017/S0022112009990863. URL https://www.cambridge.org/core/product/identifier/S0022112009990863/type/journal_article.

J. P. Gollub and Harry L. Swinney. Onset of Turbulence in a Rotating Fluid. *Physical Review Letters*, 35(14):927–930, October 1975. ISSN 0031-9007. doi: 10.1103/PhysRevLett.35.927. URL <https://link.aps.org/doi/10.1103/PhysRevLett.35.927>.

Gene H Golub and Charles F Van Loan. *Matrix computations*. JHU press, 2013. ISBN 1-4214-0859-7.

Sébastien Gomé, Laurette S. Tuckerman, and Dwight Barkley. Statistical transition to turbulence in plane channel flow. *Physical Review Fluids*, 5(8):083905, August 2020. ISSN 2469-990X. doi: 10.1103/PhysRevFluids.5.083905. URL <https://link.aps.org/doi/10.1103/PhysRevFluids.5.083905>.

Michael D. Graham and Daniel Floryan. Exact Coherent States and the Nonlinear Dynamics of Wall-Bounded Turbulent Flows. *Annual Review of Fluid Mechanics*, 53(1):227–253, January 2021. ISSN 0066-4189, 1545-4479. doi: 10.1146/annurev-fluid-051820-020223. URL <https://www.annualreviews.org/doi/10.1146/annurev-fluid-051820-020223>.

J. Halcrow, J. F. Gibson, P. Cvitanović, and D. Viswanath. Heteroclinic connections in plane Couette flow. *Journal of Fluid Mechanics*, 621:365–376, February 2009. ISSN 0022-1120, 1469-7645. doi: 10.1017/S0022112008005065. URL https://www.cambridge.org/core/product/identifier/S0022112008005065/type/journal_article.

James M. Hamilton, John Kim, and Fabian Waleffe. Regeneration mechanisms of near-wall turbulence structures. *Journal of Fluid Mechanics*, 287:317–348, March 1995. ISSN 0022-1120,

1469-7645. doi: 10.1017/S0022112095000978. URL https://www.cambridge.org/core/product/identifier/S0022112095000978/type/journal_article.

Ronald D. Henderson and Dwight Barkley. Secondary instability in the wake of a circular cylinder. *Physics of Fluids*, 8(6):1683–1685, June 1996. ISSN 1070-6631, 1089-7666. doi: 10.1063/1.868939. URL <https://pubs.aip.org/pof/article/8/6/1683/260183/Secondary-instability-in-the-wake-of-a-circular>.

Thorwald Herbert. PARABOLIZED STABILITY EQUATIONS. *Annual Review of Fluid Mechanics*, 29(1):245–283, January 1997. ISSN 0066-4189, 1545-4479. doi: 10.1146/annurev.fluid.29.1.245. URL <https://www.annualreviews.org/doi/10.1146/annurev.fluid.29.1.245>.

C.Q Hoard, C.R Robertson, and A Acrivos. Experiments on the cellular structure in bénard convection. *International Journal of Heat and Mass Transfer*, 13(5):849–856, May 1970. ISSN 00179310. doi: 10.1016/0017-9310(70)90130-4. URL <https://linkinghub.elsevier.com/retrieve/pii/0017931070901304>.

B. Hof, P. G. J. Lucas, and T. Mullin. Flow state multiplicity in convection. *Physics of Fluids*, 11(10):2815–2817, October 1999. ISSN 1070-6631, 1089-7666. doi: 10.1063/1.870178. URL <https://pubs.aip.org/pof/article/11/10/2815/254396/Flow-state-multiplicity-in-convection>.

Björn Hof, Jerry Westerweel, Tobias M. Schneider, and Bruno Eckhardt. Finite lifetime of turbulence in shear flows. *Nature*, 443(7107):59–62, September 2006. ISSN 0028-0836, 1476-4687. doi: 10.1038/nature05089. URL <https://www.nature.com/articles/nature05089>.

Eberhard Hopf. A mathematical example displaying features of turbulence. *Communications on Pure and Applied Mathematics*, 1(4):303–322, December 1948. ISSN 0010-3640, 1097-0312. doi: 10.1002/cpa.3160010401. URL <https://onlinelibrary.wiley.com/doi/10.1002/cpa.3160010401>.

M. Z. Hossain and J. M. Floryan. Drag reduction in a thermally modulated channel. *Journal of Fluid Mechanics*, 791:122–153, March 2016. ISSN 0022-1120, 1469-7645. doi: 10.1017/jfm.2016.42. URL https://www.cambridge.org/core/product/identifier/S0022112016000422/type/journal_article.

M. Z. Hossain and J. M. Floryan. On the role of surface grooves in the reduction of pressure losses in heated channels. *Physics of Fluids*, 32(8):083610, August 2020. ISSN 1070-6631, 1089-7666. doi: 10.1063/5.0018416. URL <https://pubs.aip.org/pof/article/32/8/083610/1060903/On-the-role-of-surface-grooves-in-the-reduction-of>.

M. Z. Hossain, D. Floryan, and J. M. Floryan. Drag reduction due to spatial thermal modulations. *Journal of Fluid Mechanics*, 713:398–419, December 2012. ISSN 0022-1120, 1469-7645. doi: 10.1017/jfm.2012.465. URL https://www.cambridge.org/core/product/identifier/S002211201200465X/type/journal_article.

Yuchou Hu, Robert Ecke, and Guenter Ahlers. Convection near threshold for Prandtl numbers near 1. *Physical Review E*, 48(6):4399–4413, December 1993. ISSN 1063-651X, 1095-3787. doi: 10.1103/PhysRevE.48.4399. URL <https://link.aps.org/doi/10.1103/PhysRevE.48.4399>.

Yuchou Hu, Robert Ecke, and Guenter Ahlers. Convection for Prandtl numbers near 1: Dynamics of textured patterns. *Physical Review E*, 51(4):3263–3279, April 1995. ISSN 1063-651X, 1095-3787. doi: 10.1103/PhysRevE.51.3263. URL <https://link.aps.org/doi/10.1103/PhysRevE.51.3263>.

Yuchou Hu, Robert E. Ecke, and Guenter Ahlers. Convection under rotation for Prandtl numbers near 1: Linear stability, wave-number selection, and pattern dynamics. *Physical Review E*, 55(6):6928–6949, June 1997. ISSN 1063-651X, 1095-3787. doi: 10.1103/PhysRevE.55.6928. URL <https://link.aps.org/doi/10.1103/PhysRevE.55.6928>.

Patrick Huerre and Peter A Monkewitz. Local and global instabilities in spatially developing flows. *Annual review of fluid mechanics*, 22(1):473–537, 1990. ISSN 0066-4189.

Yongyun Hwang and Carlo Cossu. Linear non-normal energy amplification of harmonic and stochastic forcing in the turbulent channel flow. *Journal of Fluid Mechanics*, 664:51–73, December 2010. ISSN 0022-1120, 1469-7645. doi: 10.1017/S0022112010003629. URL https://www.cambridge.org/core/product/identifier/S0022112010003629/type/journal_article.

O. Iida and Y. Nagano. The Relaminarization Mechanisms of Turbulent Channel Flow at Low Reynolds Numbers. *Flow, Turbulence and Combustion*, 60(2):193–213, 1998. ISSN 13866184. doi: 10.1023/A:1009999606355. URL <http://link.springer.com/10.1023/A:1009999606355>.

Harold Jeffreys. Some cases of instability in fluid motion. *Proceedings of the Royal Society of London. Series A, Containing Papers of a Mathematical and Physical Character*, 118(779):195–208, March 1928. ISSN 0950-1207, 2053-9150. doi: 10.1098/rspa.1928.0045. URL <https://royalsocietypublishing.org/doi/10.1098/rspa.1928.0045>.

Klavs F. Jensen, Erik O. Einset, and Dimitrios I. Fotiadis. Flow Phenomena in Chemical Vapor Deposition of Thin Films. *Annual Review of Fluid Mechanics*, 23(1):197–232, January 1991. ISSN 0066-4189, 1545-4479. doi: 10.1146/annurev.fl.23.010191.001213. URL <https://www.annualreviews.org/doi/10.1146/annurev.fl.23.010191.001213>.

Argyris John, Faust Gunter, and Haase Maria. Routes to chaos and turbulence. A computational introduction. *Philosophical Transactions of the Royal Society of London. Series A: Physical and Engineering Sciences*, 344(1671):207–234, August 1993. ISSN 0962-8428, 2054-0299. doi: 10.1098/rsta.1993.0088. URL <https://royalsocietypublishing.org/doi/10.1098/rsta.1993.0088>.

J. John Soundar Jerome, Jean-Marc Chomaz, and Patrick Huerre. Transient growth in Rayleigh-Bénard-Poiseuille/Couette convection. *Physics of Fluids*, 24(4):044103, April 2012. ISSN 1070-

6631, 1089-7666. doi: 10.1063/1.4704642. URL <https://pubs.aip.org/pof/article/24/4/044103/257562/Transient-growth-in-Rayleigh-Benard-Poiseuille>.

A. Karimi, Zhi-Feng Huang, and M. R. Paul. Exploring spiral defect chaos in generalized Swift-Hohenberg models with mean flow. *Physical Review E*, 84(4):046215, October 2011. ISSN 1539-3755, 1550-2376. doi: 10.1103/PhysRevE.84.046215. URL <https://link.aps.org/doi/10.1103/PhysRevE.84.046215>.

George Karniadakis and Spencer J Sherwin. *Spectral/hp element methods for computational fluid dynamics*. Oxford University Press, 2005. ISBN 0-19-852869-8.

George Em Karniadakis, Moshe Israeli, and Steven A Orszag. High-order splitting methods for the incompressible Navier-Stokes equations. *Journal of Computational Physics*, 97(2):414–443, December 1991. ISSN 00219991. doi: 10.1016/0021-9991(91)90007-8. URL <https://linkinghub.elsevier.com/retrieve/pii/0021999191900078>.

Pavan V. Kashyap, Yohann Duguet, and Olivier Dauchot. Linear Instability of Turbulent Channel Flow. *Physical Review Letters*, 129(24):244501, December 2022. ISSN 0031-9007, 1079-7114. doi: 10.1103/PhysRevLett.129.244501. URL <https://link.aps.org/doi/10.1103/PhysRevLett.129.244501>.

Genta Kawahara and Shigeo Kida. Periodic motion embedded in plane Couette turbulence: regeneration cycle and burst. *Journal of Fluid Mechanics*, 449:291–300, December 2001. ISSN 0022-1120, 1469-7645. doi: 10.1017/S0022112001006243. URL https://www.cambridge.org/core/product/identifier/S0022112001006243/type/journal_article.

R.E. Kelly. The Onset and Development of Thermal Convection in Fully Developed Shear Flows. In *Advances in Applied Mechanics*, volume 31, pages 35–112. Elsevier, 1994. ISBN 978-0-12-002031-7. doi: 10.1016/S0065-2156(08)70255-2. URL <https://linkinghub.elsevier.com/retrieve/pii/S0065215608702552>.

K.J. Kennedy and A. Zebib. Combined free and forced convection between horizontal parallel planes: some case studies. *International Journal of Heat and Mass Transfer*, 26(3):471–474, March 1983. ISSN 00179310. doi: 10.1016/0017-9310(83)90052-2. URL <https://linkinghub.elsevier.com/retrieve/pii/0017931083900522>.

R. R. Kerswell and O. R. Tutty. Recurrence of travelling waves in transitional pipe flow. *Journal of Fluid Mechanics*, 584:69–102, August 2007. ISSN 0022-1120, 1469-7645. doi: 10.1017/S0022112007006301. URL https://www.cambridge.org/core/product/identifier/S0022112007006301/type/journal_article.

T. Khapko, T. Kreilos, P. Schlatter, Y. Duguet, B. Eckhardt, and D. S. Henningson. Edge states as mediators of bypass transition in boundary-layer flows. *Journal of Fluid Mechanics*, 801:R2, August 2016. ISSN 0022-1120, 1469-7645. doi: 10.1017/jfm.2016.434. URL https://www.cambridge.org/core/product/identifier/S0022112016004341/type/journal_article.

John Kim, Parviz Moin, and Robert Moser. Turbulence statistics in fully developed channel flow at low Reynolds number. *Journal of Fluid Mechanics*, 177:133–166, April 1987. ISSN 0022-1120, 1469-7645. doi: 10.1017/S0022112087000892. URL https://www.cambridge.org/core/product/identifier/S0022112087000892/type/journal_article.

S. J. Kline, W. C. Reynolds, F. A. Schraub, and P. W. Runstadler. The structure of turbulent boundary layers. *Journal of Fluid Mechanics*, 30(4):741–773, December 1967. ISSN 0022-1120, 1469-7645. doi: 10.1017/S0022112067001740. URL https://www.cambridge.org/core/product/identifier/S0022112067001740/type/journal_article.

E.L. Koschmieder and S.G. Pallas. Heat transfer through a shallow, horizontal convecting fluid layer. *International Journal of Heat and Mass Transfer*, 17(9):991–1002, September 1974. ISSN 00179310. doi: 10.1016/0017-9310(74)90181-1. URL <https://linkinghub.elsevier.com/retrieve/pii/0017931074901811>.

Tobias Kreilos and Bruno Eckhardt. Periodic orbits near onset of chaos in plane Couette flow. *Chaos: An Interdisciplinary Journal of Nonlinear Science*, 22(4):047505, December 2012. ISSN 1054-1500, 1089-7682. doi: 10.1063/1.4757227. URL <https://pubs.aip.org/cha/article/22/4/047505/341745/Periodic-orbits-near-onset-of-chaos-in-plane>.

Ying-Cheng Lai and Tamás Tél. *Transient Chaos*, volume 173 of *Applied Mathematical Sciences*. Springer New York, New York, NY, 2011. ISBN 978-1-4419-6986-6 978-1-4419-6987-3. doi: 10.1007/978-1-4419-6987-3. URL <http://link.springer.com/10.1007/978-1-4419-6987-3>.

Lev D Landau. On the problem of turbulence. volume 44, page 311, 1944.

P. D. Lax and A. N. Milgram. IX. Parabolic Equations. In *Contributions to the Theory of Partial Differential Equations. (AM-33)*, pages 167–190. Princeton University Press, December 1955. ISBN 978-1-4008-8218-2. doi: 10.1515/9781400882182-010. URL <https://www.degruyter.com/document/doi/10.1515/9781400882182-010/html>.

P. Le Gal, A. Pocheau, and V. Croquette. Square versus Roll Pattern at Convective Threshold. *Physical Review Letters*, 54(23):2501–2504, June 1985. ISSN 0031-9007. doi: 10.1103/PhysRevLett.54.2501. URL <https://link.aps.org/doi/10.1103/PhysRevLett.54.2501>.

Richard B Lehoucq, Danny C Sorensen, and Chao Yang. *ARPACK users' guide: solution of large-scale eigenvalue problems with implicitly restarted Arnoldi methods*. SIAM, 1998. ISBN 0-89871-407-9.

Jun Liu and Guenter Ahlers. Spiral-Defect Chaos in Rayleigh-Bénard Convection with Small Prandtl Numbers. *PHYSICAL REVIEW LETTERS*, 77(15), 1996.

Mary Lowe and J. P. Gollub. Pattern Selection near the Onset of Convection: The Eckhaus Instability. *Physical Review Letters*, 55(23):2575–2578, December 1985. ISSN 0031-9007. doi: 10.1103/PhysRevLett.55.2575. URL <https://link.aps.org/doi/10.1103/PhysRevLett.55.2575>.

J-M Luijkx, Jean Karl Platten, and J Cl Legros. On the existence of thermoconvective rolls, transverse to a superimposed mean Poiseuille flow. *International Journal of Heat and Mass Transfer*, 24(7):1287–1291, 1981. ISSN 0017-9310. Publisher: Elsevier.

Dong-Jun Ma, De-Jun Sun, and Xie-Yuan Yin. Multiplicity of steady states in cylindrical Rayleigh-Bénard convection. *Physical Review E*, 74(3):037302, September 2006. ISSN 1539-3755, 1550-2376. doi: 10.1103/PhysRevE.74.037302. URL <https://link.aps.org/doi/10.1103/PhysRevE.74.037302>.

Paul Manneville. Rayleigh-Bénard Convection: Thirty Years of Experimental, Theoretical, and Modeling Work. In Gerhard Höhler, Johann H. Kühn, Thomas Müller, Joachim Trümper, Andrei Ruckenstein, Peter Wölfle, Frank Steiner, Innocent Mutabazi, José Eduardo Wesfreid, and Etienne Guyon, editors, *Dynamics of Spatio-Temporal Cellular Structures*, volume 207, pages 41–65. Springer New York, New York, NY, 2006. ISBN 978-0-387-40098-3 978-0-387-25111-0. doi: 10.1007/978-0-387-25111-0_3. URL http://link.springer.com/10.1007/978-0-387-25111-0_3. Series Title: Springer Tracts in Modern Physics.

Paul Manneville and Yves Pomeau. Intermittency and the Lorenz model. *Physics Letters A*, 75(1-2):1–2, 1979. ISSN 0375-9601. Publisher: North-Holland.

Á. Meseguer and L.N. Trefethen. Linearized pipe flow to Reynolds number 107. *Journal of Computational Physics*, 186(1):178–197, March 2003. ISSN 00219991. doi: 10.1016/S0021-9991(03)00029-9. URL <https://linkinghub.elsevier.com/retrieve/pii/S0021999103000299>.

Stephen W. Morris, Eberhard Bodenschatz, David S. Cannell, and Guenter Ahlers. Spiral defect chaos in large aspect ratio Rayleigh-Bénard convection. *Physical Review Letters*, 71(13):2026–2029, September 1993. ISSN 0031-9007. doi: 10.1103/PhysRevLett.71.2026. URL <https://link.aps.org/doi/10.1103/PhysRevLett.71.2026>.

Stephen W. Morris, Eberhard Bodenschatz, David S. Cannell, and Guenter Ahlers. The spatio-temporal structure of spiral-defect chaos. *Physica D: Nonlinear Phenomena*, 97(1-3):164–179, October 1996. ISSN 01672789. doi: 10.1016/0167-2789(96)00096-6. URL <https://linkinghub.elsevier.com/retrieve/pii/0167278996000966>.

H. W. Müller, M. Lücke, and M. Kamps. Transversal convection patterns in horizontal shear flow. *Physical Review A*, 45(6):3714–3726, March 1992. ISSN 1050-2947, 1094-1622. doi: 10.1103/PhysRevA.45.3714. URL <https://link.aps.org/doi/10.1103/PhysRevA.45.3714>.

M. Nagata. Three-dimensional finite-amplitude solutions in plane Couette flow: bifurcation from infinity. *Journal of Fluid Mechanics*, 217:519–527, August 1990. ISSN 0022-1120, 1469-7645. doi: 10.1017/S0022112090000829. URL https://www.cambridge.org/core/product/identifier/S0022112090000829/type/journal_article.

M. Nagata. Three-dimensional traveling-wave solutions in plane Couette flow. *Physical Review E*, 55(2):2023–2025, February 1997. ISSN 1063-651X, 1095-3787. doi: 10.1103/PhysRevE.55.2023. URL <https://link.aps.org/doi/10.1103/PhysRevE.55.2023>.

X. Nicolas, A. Mojtabi, and J. K. Platten. Two-dimensional numerical analysis of the Poiseuille–Bénard flow in a rectangular channel heated from below. *Physics of Fluids*, 9(2):337–348, February 1997. ISSN 1070-6631, 1089-7666. doi: 10.1063/1.869235. URL <https://pubs.aip.org/pof/article/9/2/337/259822/Two-dimensional-numerical-analysis-of-the>.

X. Nicolas, J.-M. Luijkx, and J.-K. Platten. Linear stability of mixed convection flows in horizontal rectangular channels of finite transversal extension heated from below. *International Journal of Heat and Mass Transfer*, 43(4):589–610, February 2000. ISSN 00179310. doi: 10.1016/S0017-9310(99)00099-X. URL <https://linkinghub.elsevier.com/retrieve/pii/S001793109900099X>.

Xavier Nicolas. Revue bibliographique sur les écoulements de Poiseuille–Rayleigh–Bénard : écoulements de convection mixte en conduites rectangulaires horizontales chauffées par le bas. *International Journal of Thermal Sciences*, 41(10):961–1016, October 2002. ISSN 12900729. doi: 10.1016/S1290-0729(02)01374-1. URL <https://linkinghub.elsevier.com/retrieve/pii/S1290072902013741>.

Xavier Nicolas, Shihe Xin, and Noussaiba Zoueidi. Characterisation of a Wavy Convective Instability in Poiseuille-Rayleigh-Be’nard Flows: Linear Stability Analysis and Non Linear Numerical Simulations Under Random Excitations. In *2010 14th International Heat Transfer Conference, Volume 7*, pages 203–208, Washington, DC, USA, January 2010. ASMEDC. ISBN 978-0-7918-4942-2 978-0-7918-3879-2. doi: 10.1115/IHTC14-22256. URL <https://asmedigitalcollection.asme.org/IHTC/proceedings/IHTC14/49422/203/360332>.

Xavier Nicolas, Noussaiba Zoueidi, and Shihe Xin. Influence of a white noise at channel inlet on the parallel and wavy convective instabilities of Poiseuille-Rayleigh-Bénard flows. *Physics of Fluids*, 24(8):084101, August 2012. ISSN 1070-6631, 1089-7666. doi: 10.1063/1.4737652. URL <https://pubs.aip.org/pof/article/24/8/084101/258132/Influence-of-a-white-noise-at-channel-inlet-on-the>.

William M’F. Orr. The Stability or Instability of the Steady Motions of a Perfect Liquid and of a Viscous Liquid. Part II: A Viscous Liquid. *Proceedings of the Royal Irish Academy. Section A: Mathematical and Physical Sciences*, 27:69–138, 1907. ISSN 00358975. URL <http://www.jstor.org/stable/20490591>. Publisher: Royal Irish Academy.

Steven A. Orszag. Accurate solution of the Orr–Sommerfeld stability equation. *Journal of Fluid Mechanics*, 50(4):689–703, December 1971. ISSN 0022-1120, 1469-7645. doi: 10.1017/S0022112071002842. URL https://www.cambridge.org/core/product/identifier/S0022112071002842/type/journal_article.

Steven A. Orszag and Anthony T. Patera. Secondary instability of wall-bounded shear flows. *Journal of Fluid Mechanics*, 128(-1):347, March 1983. ISSN 0022-1120, 1469-7645.

doi: 10.1017/S0022112083000518. URL http://www.journals.cambridge.org/abstract_S0022112083000518.

Steven A. Orszag, Moshe Israeli, and Michel O. Deville. Boundary conditions for incompressible flows. *Journal of Scientific Computing*, 1(1):75–111, 1986. ISSN 0885-7474, 1573-7691. doi: 10.1007/BF01061454. URL <http://link.springer.com/10.1007/BF01061454>.

S. Ostrach and Y. Kamotani. Heat Transfer Augmentation in Laminar Fully Developed Channel Flow by Means of Heating From Below. *Journal of Heat Transfer*, 97(2):220–225, May 1975. ISSN 0022-1481, 1528-8943. doi: 10.1115/1.3450344. URL <https://asmedigitalcollection.asme.org/heattransfer/article/97/2/220/416581/Heat-Transfer-Augmentation-in-Laminar-Fully>.

MT Ouazzani, Jean-Paul Caltagirone, Gilles Meyer, and Abdelkader Mojtabi. Etude numerique et expérimentale de la convection mixte entre deux plans horizontaux à températures différentes. *International journal of heat and mass transfer*, 32(2):261–269, 1989. ISSN 0017-9310. Publisher: Elsevier.

MT Ouazzani, Jean Karl Platten, and Abdelkader Mojtabi. Etude expérimentale de la convection mixte entre deux plans horizontaux à températures différentes—II. *International journal of heat and mass transfer*, 33(7):1417–1427, 1990. ISSN 0017-9310. Publisher: Elsevier.

Hervé Pabiou, Xavier Nicolas, Shihe Xin, and Sophie Mergui. Observations d'une instabilité convective apparaissant sous la forme de rouleaux sinueux dans un écoulement de Poiseuille–Rayleigh–Bénard. *Mécanique & industries*, 4(5):537–543, 2003. ISSN 1296-2139. Publisher: Elsevier.

Hervé Pabiou, Sophie Mergui, and Christine Bénard. Wavy secondary instability of longitudinal rolls in RayleighPoiseuille flows. *Journal of Fluid Mechanics*, 542(-1):175, October 2005. ISSN 0022-1120, 1469-7645. doi: 10.1017/S0022112005006154. URL http://www.journals.cambridge.org/abstract_S0022112005006154.

Chaitanya S Paranjape. Onset of turbulence in plane Poiseuille flow. 2019. Publisher: IST Austria Klosterneuburg, Austria.

Chaitanya S. Paranjape, Yohann Duguet, and Björn Hof. Oblique stripe solutions of channel flow. *Journal of Fluid Mechanics*, 897:A7, August 2020. ISSN 0022-1120, 1469-7645. doi: 10.1017/jfm.2020.322. URL https://www.cambridge.org/core/product/identifier/S0022112020003225/type/journal_article.

Chaitanya S. Paranjape, Gökhan Yalnız, Yohann Duguet, Nazmi Burak Budanur, and Björn Hof. Direct Path from Turbulence to Time-Periodic Solutions. *Physical Review Letters*, 131(3):034002, July 2023. ISSN 0031-9007, 1079-7114. doi: 10.1103/PhysRevLett.131.034002. URL <https://link.aps.org/doi/10.1103/PhysRevLett.131.034002>.

V. C. Patel and M. R. Head. Some observations on skin friction and velocity profiles in fully developed pipe and channel flows. *Journal of Fluid Mechanics*, 38(1):181–201, August 1969. ISSN 0022-1120, 1469-7645. doi: 10.1017/S0022112069000115. URL https://www.cambridge.org/core/product/identifier/S0022112069000115/type/journal_article.

Anthony T Patera. A spectral element method for fluid dynamics: Laminar flow in a channel expansion. *Journal of Computational Physics*, 54(3):468–488, June 1984. ISSN 00219991. doi: 10.1016/0021-9991(84)90128-1. URL <https://linkinghub.elsevier.com/retrieve/pii/0021999184901281>.

M. R. Paul, M. I. Einarsson, P. F. Fischer, and M. C. Cross. Extensive chaos in Rayleigh-Bénard convection. *Physical Review E*, 75(4):045203, April 2007. ISSN 1539-3755, 1550-2376. doi: 10.1103/PhysRevE.75.045203. URL <https://link.aps.org/doi/10.1103/PhysRevE.75.045203>.

M.R. Paul, K.-H. Chiam, M.C. Cross, P.F. Fischer, and H.S. Greenside. Pattern formation and dynamics in Rayleigh–Bénard convection: numerical simulations of experimentally realistic geometries. *Physica D: Nonlinear Phenomena*, 184(1-4):114–126, October 2003. ISSN 01672789. doi: 10.1016/S0167-2789(03)00216-1. URL <https://linkinghub.elsevier.com/retrieve/pii/S0167278903002161>.

Anne Pellew and Richard Vynne Southwell. On maintained convective motion in a fluid heated from below. *Proceedings of the Royal Society of London. Series A. Mathematical and Physical Sciences*, 176(966):312–343, November 1940. ISSN 0080-4630, 2053-9169. doi: 10.1098/rspa.1940.0092. URL <https://royalsocietypublishing.org/doi/10.1098/rspa.1940.0092>.

Sergio Pirozzoli, Matteo Bernardini, Roberto Verzicco, and Paolo Orlandi. Mixed convection in turbulent channels with unstable stratification. *Journal of Fluid Mechanics*, 821:482–516, June 2017. ISSN 0022-1120, 1469-7645. doi: 10.1017/jfm.2017.216. URL https://www.cambridge.org/core/product/identifier/S0022112017002166/type/journal_article.

Brendan B Plapp and Eberhard Bodenschatz. Core dynamics of multi-armed spirals in Rayleigh–Bénard convection. *Physica Scripta*, T67:111–116, January 1996. ISSN 0031-8949, 1402-4896. doi: 10.1088/0031-8949/1996/T67/022. URL <https://iopscience.iop.org/article/10.1088/0031-8949/1996/T67/022>.

Brendan B. Plapp, David A. Egolf, Eberhard Bodenschatz, and Werner Pesch. Dynamics and Selection of Giant Spirals in Rayleigh-Bénard Convection. *Physical Review Letters*, 81(24):5334–5337, December 1998. ISSN 0031-9007, 1079-7114. doi: 10.1103/PhysRevLett.81.5334. URL <https://link.aps.org/doi/10.1103/PhysRevLett.81.5334>.

Brendan Bryce Plapp. Spiral pattern formation in Rayleigh-Benard convection. *Ph.D. Thesis*, page 3118, December 1997. URL <https://ui.adsabs.harvard.edu/abs/1997PhDT.....105P>.

A. Prigent and O. Dauchot. "Barber pole turbulence" in large aspect ratio Taylor-Couette flow. *Physical Review Letters*, 89(1):014501, June 2002. ISSN 0031-9007, 1079-7114. doi: 10.1103/PhysRevLett.89.014501. URL <http://arxiv.org/abs/cond-mat/0009241>. arXiv:cond-mat/0009241.

Arnaud Prigent, Guillaume Grégoire, Hugues Chaté, and Olivier Dauchot. Long-wavelength modulation of turbulent shear flows. *Physica D: Nonlinear Phenomena*, 174(1-4):100–113, January 2003. ISSN 01672789. doi: 10.1016/S0167-2789(02)00685-1. URL <https://linkinghub.elsevier.com/retrieve/pii/S0167278902006851>.

Chris C.T Pringle, Yohann Duguet, and Rich R Kerswell. Highly symmetric travelling waves in pipe flow. *Philosophical Transactions of the Royal Society A: Mathematical, Physical and Engineering Sciences*, 367(1888):457–472, February 2009. ISSN 1364-503X, 1471-2962. doi: 10.1098/rsta.2008.0236. URL <https://royalsocietypublishing.org/doi/10.1098/rsta.2008.0236>.

Gregory Pujals, Manuel García-Villalba, Carlo Cossu, and Sébastien Depardon. A note on optimal transient growth in turbulent channel flows. *Physics of Fluids*, 21(1):015109, January 2009. ISSN 1070-6631, 1089-7666. doi: 10.1063/1.3068760. URL <https://pubs.aip.org/pof/article/21/1/015109/256743/A-note-on-optimal-transient-growth-in-turbulent>.

Subhashis Ray and J. Srinivasan. Analysis of conjugate laminar mixed convection cooling in a shrouded array of electronic components. *International Journal of Heat and Mass Transfer*, 35(4):815–822, April 1992. ISSN 00179310. doi: 10.1016/0017-9310(92)90249-R. URL <https://linkinghub.elsevier.com/retrieve/pii/001793109290249R>.

Lord Rayleigh. LIX. *On convection currents in a horizontal layer of fluid, when the higher temperature is on the under side. The London, Edinburgh, and Dublin Philosophical Magazine and Journal of Science*, 32(192):529–546, December 1916. ISSN 1941-5982, 1941-5990. doi: 10.1080/14786441608635602. URL <https://www.tandfonline.com/doi/full/10.1080/14786441608635602>.

Satish C. Reddy and Dan S. Henningson. Energy growth in viscous channel flows. *Journal of Fluid Mechanics*, 252:209–238, July 1993. ISSN 0022-1120, 1469-7645. doi: 10.1017/S0022112093003738. URL https://www.cambridge.org/core/product/identifier/S0022112093003738/type/journal_article.

Satish C. Reddy, Peter J. Schmid, and Dan S. Henningson. Pseudospectra of the Orr–Sommerfeld Operator. *SIAM Journal on Applied Mathematics*, 53(1):15–47, February 1993. ISSN 0036-1399, 1095-712X. doi: 10.1137/0153002. URL <http://pubs.siam.org/doi/10.1137/0153002>.

Florian Reetz and Tobias M. Schneider. Invariant states in inclined layer convection. Part 1. Temporal transitions along dynamical connections between invariant states. *Journal of Fluid Mechanics*, 898:A22, September 2020. ISSN 0022-1120, 1469-7645. doi: 10.1017/jfm.2020.317. URL https://www.cambridge.org/core/product/identifier/S0022112020003171/type/journal_article.

Florian Reetz, Tobias Kreilos, and Tobias M. Schneider. Exact invariant solution reveals the origin of self-organized oblique turbulent-laminar stripes. *Nature Communications*, 10(1):2277, May 2019. ISSN 2041-1723. doi: 10.1038/s41467-019-10208-x. URL <https://doi.org/10.1038/s41467-019-10208-x>.

Florian Reetz, Priya Subramanian, and Tobias M. Schneider. Invariant states in inclined layer convection. Part 2. Bifurcations and connections between branches of invariant states. *Journal of Fluid Mechanics*, 898:A23, September 2020. ISSN 0022-1120, 1469-7645. doi: 10.1017/jfm.2020.318. URL https://www.cambridge.org/core/product/identifier/S0022112020003183/type/journal_article.

Osborne Reynolds. XXIX. An experimental investigation of the circumstances which determine whether the motion of water shall be direct or sinuous, and of the law of resistance in parallel channels. *Philosophical Transactions of the Royal Society of London*, 174:935–982, December 1883. ISSN 0261-0523, 2053-9223. doi: 10.1098/rstl.1883.0029. URL <https://royalsocietypublishing.org/doi/10.1098/rstl.1883.0029>.

Osborne Reynolds. IV. On the dynamical theory of incompressible viscous fluids and the determination of the criterion. *Philosophical Transactions of the Royal Society of London. (A.)*, 186:123–164, December 1895. ISSN 0264-3820, 2053-9231. doi: 10.1098/rsta.1895.0004. URL <https://royalsocietypublishing.org/doi/10.1098/rsta.1895.0004>.

Gabriele Rocco. Advanced Instability Methods using Spectral/hp Discretisations and their Applications to Complex Geometries. 2014.

H. T. Rossby. A study of Bénard convection with and without rotation. *Journal of Fluid Mechanics*, 36(2):309–335, April 1969. ISSN 0022-1120, 1469-7645. doi: 10.1017/S0022112069001674. URL https://www.cambridge.org/core/product/identifier/S0022112069001674/type/journal_article.

David Ruelle and Floris Takens. On the nature of turbulence. *Communications in Mathematical Physics*, 20(3):167–192, September 1971. ISSN 0010-3616, 1432-0916. doi: 10.1007/BF01646553. URL <http://link.springer.com/10.1007/BF01646553>.

Sten Rüdiger and Fred Feudel. Pattern formation in Rayleigh-Bénard convection in a cylindrical container. *Physical Review E*, 62(4):4927–4931, October 2000. ISSN 1063-651X, 1095-3787. doi: 10.1103/PhysRevE.62.4927. URL <https://link.aps.org/doi/10.1103/PhysRevE.62.4927>.

A. Scagliarini, H. Einarsson, Á. Gylfason, and F. Toschi. Law of the wall in an unstably stratified turbulent channel flow. *Journal of Fluid Mechanics*, 781:R5, October 2015. ISSN 0022-1120, 1469-7645. doi: 10.1017/jfm.2015.498. URL https://www.cambridge.org/core/product/identifier/S002211201500498X/type/journal_article.

Andrea Scagliarini, Armann Gylfason, and Federico Toschi. Heat flux scaling in turbulent Rayleigh-Bénard convection with an imposed longitudinal wind. *Physical Review E*, 89(4):043012, April 2014. ISSN 1539-3755, 1550-2376. doi: 10.1103/PhysRevE.89.043012. URL <http://arxiv.org/abs/1311.4598>. arXiv:1311.4598 [physics].

H. Schlichting. Zur Entstehung der Turbulenz bei der Plattenströmung. *Nachrichten von der Gesellschaft der Wissenschaften zu Göttingen, Mathematisch-Physikalische Klasse*, 1933:181–208, 1933. URL <http://eudml.org/doc/59420>.

Hermann Schlichting and Klaus Gersten. Onset of Turbulence (Stability Theory). In *Boundary-Layer Theory*, pages 415–496. Springer Berlin Heidelberg, Berlin, Heidelberg, 2017. ISBN 978-3-662-52917-1 978-3-662-52919-5. doi: 10.1007/978-3-662-52919-5_15. URL http://link.springer.com/10.1007/978-3-662-52919-5_15.

A. Schlüter, D. Lortz, and F. Busse. On the stability of steady finite amplitude convection. *Journal of Fluid Mechanics*, 23(01):129, September 1965. ISSN 0022-1120, 1469-7645. doi: 10.1017/S0022112065001271. URL http://www.journals.cambridge.org/abstract_S0022112065001271.

Peter J. Schmid. Nonmodal Stability Theory. *Annual Review of Fluid Mechanics*, 39(1):129–162, January 2007. ISSN 0066-4189, 1545-4479. doi: 10.1146/annurev.fluid.38.050304.092139. URL <https://www.annualreviews.org/doi/10.1146/annurev.fluid.38.050304.092139>.

Peter J. Schmid and Dan S. Henningson. *Stability and Transition in Shear Flows*, volume 142 of *Applied Mathematical Sciences*. Springer New York, New York, NY, 2001. ISBN 978-1-4612-6564-1 978-1-4613-0185-1. doi: 10.1007/978-1-4613-0185-1. URL <http://link.springer.com/10.1007/978-1-4613-0185-1>.

Rainer Schmitz, Werner Pesch, and Walter Zimmermann. Spiral-defect chaos: Swift-Hohenberg model versus Boussinesq equations. *Physical Review E*, 65(3):037302, March 2002. ISSN 1063-651X, 1095-3787. doi: 10.1103/PhysRevE.65.037302. URL <https://link.aps.org/doi/10.1103/PhysRevE.65.037302>.

Tobias M Schneider and Bruno Eckhardt. Edge states intermediate between laminar and turbulent dynamics in pipe flow. *Philosophical Transactions of the Royal Society A: Mathematical, Physical and Engineering Sciences*, 367(1888):577–587, February 2009. ISSN 1364-503X, 1471-2962. doi: 10.1098/rsta.2008.0216. URL <https://royalsocietypublishing.org/doi/10.1098/rsta.2008.0216>.

Tobias M. Schneider, Bruno Eckhardt, and James A. Yorke. Turbulence transition and the edge of chaos in pipe flow. *Physical Review Letters*, 99(3):034502, July 2007. ISSN 0031-9007, 1079-7114. doi: 10.1103/PhysRevLett.99.034502. URL <http://arxiv.org/abs/nlin/0703067>. arXiv:nlin/0703067.

Masaki Shimizu and Paul Manneville. Bifurcations to turbulence in transitional channel flow. *Physical Review Fluids*, 4(11):113903, November 2019. doi: 10.1103/PhysRevFluids.4.113903. URL <https://link.aps.org/doi/10.1103/PhysRevFluids.4.113903>. Publisher: American Physical Society.

Jennifer H. Siggers. Dynamics of target patterns in low-Prandtl-number convection. *Journal of Fluid Mechanics*, 475:357–375, January 2003. ISSN 0022-1120, 1469-7645. doi: 10.1017/S0022112002002896. URL https://www.cambridge.org/core/product/identifier/S0022112002002896/type/journal_article.

Joseph D. Skufca, James A. Yorke, and Bruno Eckhardt. Edge of Chaos in a Parallel Shear Flow. *Physical Review Letters*, 96(17):174101, May 2006. ISSN 0031-9007, 1079-7114. doi: 10.1103/PhysRevLett.96.174101. URL <https://link.aps.org/doi/10.1103/PhysRevLett.96.174101>.

C. R. Smith and S. P. Metzler. The characteristics of low-speed streaks in the near-wall region of a turbulent boundary layer. *Journal of Fluid Mechanics*, 129(-1):27, April 1983. ISSN 0022-1120, 1469-7645. doi: 10.1017/S0022112083000634. URL http://www.journals.cambridge.org/abstract_S0022112083000634.

Arnold Sommerfeld. *Ein Beitrag zur hydrodynamischen Erklarung der turbulenten Flussigkeitsbewegungen*. 1909.

Baofang Song, Dwight Barkley, Bjorn Hof, and Marc Avila. Speed and structure of turbulent fronts in pipe flow. *Journal of Fluid Mechanics*, 813:1045–1059, February 2017. ISSN 0022-1120, 1469-7645. doi: 10.1017/jfm.2017.14. URL https://www.cambridge.org/core/product/identifier/S0022112017000143/type/journal_article.

Herbert Brian Squire. On the stability for three-dimensional disturbances of viscous fluid flow between parallel walls. *Proceedings of the Royal Society of London. Series A, Containing Papers of a Mathematical and Physical Character*, 142(847):621–628, November 1933. ISSN 0950-1207, 2053-9150. doi: 10.1098/rspa.1933.0193. URL <https://royalsocietypublishing.org/doi/10.1098/rspa.1933.0193>.

J. Swift and P. C. Hohenberg. Hydrodynamic fluctuations at the convective instability. *Physical Review A*, 15(1):319–328, January 1977. ISSN 0556-2791. doi: 10.1103/PhysRevA.15.319. URL <https://link.aps.org/doi/10.1103/PhysRevA.15.319>.

Harry L Swinney and Jerry P Gollub. The transition to turbulence. *Physics today*, 31(8):41–49, 1978. ISSN 0031-9228. Publisher: American Institute of Physics.

J. J. Tao, Bruno Eckhardt, and X. M. Xiong. Extended localized structures and the onset of turbulence in channel flow. *Physical Review Fluids*, 3(1):011902, January 2018. doi: 10.1103/PhysRevFluids.3.011902. URL <https://link.aps.org/doi/10.1103/PhysRevFluids.3.011902>. Publisher: American Physical Society.

Vassilios Theoflis. Advances in global linear instability analysis of nonparallel and three-dimensional flows. *Progress in Aerospace Sciences*, 39(4):249–315, May 2003. ISSN 03760421. doi: 10.1016/S0376-0421(02)00030-1. URL <https://linkinghub.elsevier.com/retrieve/pii/S0376042102000301>.

Sadayoshi Toh and Tomoaki Itano. A periodic-like solution in channel flow. *Journal of Fluid Mechanics*, 481:67–76, April 2003. ISSN 00221120, 14697645. doi: 10.1017/S0022112003003768. URL http://www.journals.cambridge.org/abstract_S0022112003003768.

W. Tollmien. Über die Entstehung der Turbulenz. 1. Mitteilung. *Nachrichten von der Gesellschaft der Wissenschaften zu Göttingen, Mathematisch-Physikalische Klasse*, 1929:21–44, 1928. URL <http://eudml.org/doc/59276>.

Lloyd N. Trefethen. Pseudospectra of Linear Operators. *SIAM Review*, 39(3):383–406, January 1997. ISSN 0036-1445, 1095-7200. doi: 10.1137/S0036144595295284. URL <http://pubs.siam.org/doi/10.1137/S0036144595295284>.

Takahiro Tsukahara, Kaoru Iwamoto, Hiroshi Kawamura, and Tetsuaki Takeda. DNS of heat transfer in a transitional channel flow accompanied by a turbulent puff-like structure, September 2014a. URL <http://arxiv.org/abs/1406.0586>. arXiv:1406.0586 [physics].

Takahiro Tsukahara, Yasuo Kawaguchi, and Hiroshi Kawamura. An experimental study on turbulent-stripe structure in transitional channel flow, 2014b. URL <https://arxiv.org/abs/1406.1378>. Version Number: 2.

Takahiro Tsukahara, Yohji Seki, Hiroshi Kawamura, and Daisuke Tochio. DNS of turbulent channel flow at very low Reynolds numbers, September 2014c. URL <http://arxiv.org/abs/1406.0248>. arXiv:1406.0248 [physics].

Laurette S. Tuckerman and Dwight Barkley. Global Bifurcation to Traveling Waves in Axisymmetric Convection. *Physical Review Letters*, 61(4):408–411, July 1988. ISSN 0031-9007. doi: 10.1103/PhysRevLett.61.408. URL <https://link.aps.org/doi/10.1103/PhysRevLett.61.408>.

Laurette S. Tuckerman and Dwight Barkley. Bifurcation Analysis for Timesteppers. In *Numerical Methods for Bifurcation Problems and Large-Scale Dynamical Systems*, volume 119, pages 453–466. Springer New York, New York, NY, 2000. ISBN 978-1-4612-7044-7 978-1-4612-1208-9. doi: 10.1007/978-1-4612-1208-9_20. URL http://link.springer.com/10.1007/978-1-4612-1208-9_20. Series Title: The IMA Volumes in Mathematics and its Applications.

Laurette S Tuckerman and Dwight Barkley. Patterns and dynamics in transitional plane Couette flow. *Physics of Fluids*, 23(4), 2011. ISSN 1070-6631. Publisher: AIP Publishing.

Laurette S. Tuckerman, Tobias Kreilos, Hecke Schröbsdorff, Tobias M. Schneider, and John F. Gibson. Turbulent-laminar patterns in plane Poiseuille flow. *Physics of Fluids*, 26(11):114103, November 2014. ISSN 1070-6631, 1089-7666. doi: 10.

1063/1.4900874. URL <https://pubs.aip.org/pof/article/26/11/114103/315350/Turbulent-laminar-patterns-in-plane-Poiseuille>.

R. Temam. Sur l'approximation de la solution des équations de Navier-Stokes par la méthode des pas fractionnaires (II). *Archive for Rational Mechanics and Analysis*, 33(5):377–385, January 1969. ISSN 0003-9527, 1432-0673. doi: 10.1007/BF00247696. URL <http://link.springer.com/10.1007/BF00247696>.

Geoffrey K. Vallis, Douglas J. Parker, and Steven M. Tobias. A simple system for moist convection: the Rainy-Bénard model. *Journal of Fluid Mechanics*, 862:162–199, March 2019. ISSN 0022-1120, 1469-7645. doi: 10.1017/jfm.2018.954. URL https://www.cambridge.org/core/product/identifier/S0022112018009540/type/journal_article.

Milton Van Dyke and Milton Van Dyke. *An album of fluid motion*, volume 176. Parabolic Press Stanford, 1982.

D. Viswanath. Recurrent motions within plane Couette turbulence. *Journal of Fluid Mechanics*, 580:339–358, June 2007. ISSN 0022-1120, 1469-7645. doi: 10.1017/S0022112007005459. URL https://www.cambridge.org/core/product/identifier/S0022112007005459/type/journal_article.

Eduardo Vitral, Saikat Mukherjee, Perry H. Leo, Jorge Viñals, Mark R. Paul, and Zhi-Feng Huang. Spiral defect chaos in Rayleigh-Bénard convection: Asymptotic and numerical studies of azimuthal flows induced by rotating spirals. *Physical Review Fluids*, 5(9):093501, September 2020. ISSN 2469-990X. doi: 10.1103/PhysRevFluids.5.093501. URL <https://link.aps.org/doi/10.1103/PhysRevFluids.5.093501>.

Fabian Waleffe. Exact coherent structures in channel flow. *Journal of Fluid Mechanics*, 435:93–102, May 2001. ISSN 0022-1120, 1469-7645. doi: 10.1017/S0022112001004189. URL https://www.cambridge.org/core/product/identifier/S0022112001004189/type/journal_article.

Fabian Waleffe. Homotopy of exact coherent structures in plane shear flows. *Physics of Fluids*, 15(6):1517–1534, June 2003. ISSN 1070-6631, 1089-7666. doi: 10.1063/1.1566753. URL <https://pubs.aip.org/pof/article/15/6/1517/448391/Homotopy-of-exact-coherent-structures-in-plane>.

Jue Wang, John Gibson, and Fabian Waleffe. Lower Branch Coherent States in Shear Flows: Transition and Control. *Physical Review Letters*, 98(20):204501, May 2007. ISSN 0031-9007, 1079-7114. doi: 10.1103/PhysRevLett.98.204501. URL <https://link.aps.org/doi/10.1103/PhysRevLett.98.204501>.

H. Wedin and R. R. Kerswell. Exact coherent structures in pipe flow: travelling wave solutions. *Journal of Fluid Mechanics*, 508:333–371, June 2004. ISSN 0022-1120, 1469-7645.

doi: 10.1017/S0022112004009346. URL http://www.journals.cambridge.org/abstract_S0022112004009346.

José Eduardo Wesfreid. Henri Bénard: Thermal convection and vortex shedding. *Comptes Rendus. Mécanique*, 345(7):446–466, June 2017. ISSN 1873-7234. doi: 10.1016/j.crme.2017.06.006. URL <https://comptes-rendus.academie-sciences.fr/mecanique/articles/10.1016/j.crme.2017.06.006/>.

G. E. Willis and J. W. Deardorff. The oscillatory motions of Rayleigh convection. *Journal of Fluid Mechanics*, 44(04):661, December 1970. ISSN 0022-1120, 1469-7645. doi: 10.1017/S0022112070002070. URL http://www.journals.cambridge.org/abstract_S0022112070002070.

Hao-wen Xi, J. D. Gunton, and Jorge Viñals. Spiral defect chaos in a model of Rayleigh-Bénard convection. *Physical Review Letters*, 71(13):2030–2033, September 1993. ISSN 0031-9007. doi: 10.1103/PhysRevLett.71.2030. URL <https://link.aps.org/doi/10.1103/PhysRevLett.71.2030>.

Haowen Xi and J. D. Gunton. Spatiotemporal chaos in a model of Rayleigh-Bénard convection. *Physical Review E*, 52(5):4963–4975, November 1995. ISSN 1063-651X, 1095-3787. doi: 10.1103/PhysRevE.52.4963. URL <https://link.aps.org/doi/10.1103/PhysRevE.52.4963>.

Xiangkai Xiao and Baofang Song. The growth mechanism of turbulent bands in channel flow at low Reynolds numbers. *Journal of Fluid Mechanics*, 883:R1, January 2020. ISSN 0022-1120, 1469-7645. doi: 10.1017/jfm.2019.899. URL https://www.cambridge.org/core/product/identifier/S0022112019008991/type/journal_article.

Shihe Xin, Xavier Nicolas, and Patrick Le Quéré. Stability analyses of Longitudinal Rolls of Poiseuille-Rayleigh-Bénard Flows in Air-Filled Channels of Finite Transversal Extension. *Numerical Heat Transfer, Part A: Applications*, 50(5):467–490, July 2006. ISSN 1040-7782, 1521-0634. doi: 10.1080/10407780600620079. URL <http://www.tandfonline.com/doi/abs/10.1080/10407780600620079>.

Xiangming Xiong, Jianjun Tao, Shiyi Chen, and Luca Brandt. Turbulent bands in plane-Poiseuille flow at moderate Reynolds numbers. *Physics of Fluids*, 27(4):041702, April 2015. ISSN 1070-6631, 1089-7666. doi: 10.1063/1.4917173. URL <https://pubs.aip.org/pof/article/27/4/041702/1019208/Turbulent-bands-in-plane-Poiseuille-flow-at>.

Stefan Zammert and Bruno Eckhardt. Crisis bifurcations in plane Poiseuille flow. *Physical Review E*, 91(4):041003, April 2015. ISSN 1539-3755, 1550-2376. doi: 10.1103/PhysRevE.91.041003. URL <https://link.aps.org/doi/10.1103/PhysRevE.91.041003>.